



Integrated Project - EUWB

Contract No 215669

Deliverable

D4.4.1b

**Analysis of the impact of location information on communication systems
(final)**

Contractual data:	M24
Actual data:	M26
Authors:	Stefano Severi, Andrea Giorgetti, Davide Dardari, Juan Chóliz, Ángela Hernández, Golaleh Rahmatollahi, Giuseppe Abreu
Participants:	UNIBO, CWC, LUH, UZ
Work package:	WP4
Security:	PU
Nature:	Report
Version:	1.0
Total number of pages:	62

Abstract

This document describes the theoretical limits in ranging and localization and provides a study on the impact of location information on the communications

Keywords

UWB, Ranging, Localization, Location Information, Transmission Capacity, Cognitive Radio, Interference

Table of Contents

1 Executive summary	9
2 Impact of Location Information on Communication.....	10
2.1 RSSI-based Localization of Unknown Targets\Interferers	10
2.1.1 Scenario Description	10
2.1.2 Model Description.....	11
2.1.2.1 WiFi Channel Model	11
2.1.2.2 Locating the Interferer.....	11
2.1.3 Simulation results	13
2.1.4 Future Research Directions	15
2.1.5 Conclusion.....	16
2.2 Analysis of Combined Communication and Tracking Systems.....	16
2.2.1 Introduction	16
2.2.2 System description	17
2.2.2.1 MAC layer description	17
2.2.2.2 LT system description	20
2.2.2.3 Tracking Function Distribution in the Network	22
2.2.2.4 Simulator description	22
2.2.2.5 Ranging model	23
2.2.2.6 Tracking algorithms	24
2.2.3 Analysis and evaluation.....	25
2.2.3.1 Data acquisition & distribution enhancements.....	25
2.2.3.2 Impact of the tracking system architecture.....	34
2.2.3.3 Conclusions	44
2.2.4 Impact on Radio Resource Management.....	45

2.3 Policy-Dependent distance distribution in linear multi-hop ad hoc networks.....	46
2.3.1 Single and multi-hop distances.....	47
2.3.1.1 Single-hop statistics.....	48
2.3.1.2 Multi-hop statistics	49
2.3.2 Average number of hops	52
2.3.3 Probability distribution of the number of hops.....	54
2.3.4 Evaluation and simulation results.....	56
2.3.5 Conclusion.....	59
References	60
Acknowledgement.....	62

List of Figures

Figure 1: Target position estimation for different value of path-loss factor.....	14
Figure 2: Target Localization Error (in meters) for different value of path-loss factor and different shadowing levels.....	15
Figure 3: EUWB MAC superframe structure [11].....	19
Figure 4: Mesh centralized topology [11].....	19
Figure 5: Example of meshed scheduling tree [11].....	20
Figure 6: UWB location simulator scenario.....	22
Figure 7. Update process scheme for 1LC SRq SRp NDA depending on the number of anchors.....	26
Figure 8. Update process scheme for 1LC MRq SRp NDA depending on the number of anchors.....	26
Figure 9. Update process scheme for 1LC SRq SRp DA depending on the number of anchors.....	27
Figure 10. Update process scheme for 1LC MRq SRp DA depending on the number of anchors.....	27
Figure 11: Average error for different acquisition & distribution modes depending on the number of anchors for location.....	28
Figure 12: Number of slots per update for different acquisition & distribution modes depending on the number of anchors for location.....	29
Figure 13: Data slots available for communication for different acquisition & distribution modes depending on the number of anchors for location.....	29
Figure 14. Update process scheme for 1LC SRq SRp NDA depending on the number of targets.....	30
Figure 15. Update process scheme for 1LC SRq SRp DA depending on the number of targets.....	30
Figure 16. Update process scheme for 1LC MRq SRp DA depending on the number of targets.....	31
Figure 17. Update process scheme for 1LC MRq MRp DA depending on the number of targets.....	31
Figure 18: Average error for different acquisition & distribution modes depending on the number of targets.....	32
Figure 19: Time between updates for different acquisition & distribution modes depending on the number of targets.....	33
Figure 20: Data slots available for communication for different acquisition & distribution modes depending on the number of targets.....	33
Figure 21: Ranging slots used for different acquisition & distribution modes depending on the number of targets.....	34
Figure 22. Update process scheme for Distributed SRq SRp NDA depending on the number of anchors.....	34
Figure 23. Update process scheme for Mobile SRq SRp NDA depending on the number of anchors.....	35
Figure 24: Average error for different tracking architectures depending on the number of anchors for location (mode SRq SRp NDA).....	35

Figure 25: Number of slots per update for different tracking architectures depending on the number of anchors for location (mode SRq SRp NDA)	36
Figure 26: Data slots available for communication for different tracking architectures depending on the number of anchors for location (mode SRq SRp NDA)	36
Figure 27. Update process scheme for Distributed SRq SRp NDA depending on the number of targets	37
Figure 28. Update process scheme for Mobile SRq SRp NDA depending on the number of targets ...	37
Figure 29: Average error for different tracking architectures depending on the number of targets (mode SRq SRp NDA)	38
Figure 30: Time between updates for different tracking architectures depending on the number of targets (mode SRq SRp NDA).....	38
Figure 31: Data slots available for communication for different tracking architectures depending on the number of targets (mode SRq SRp NDA)	39
Figure 32: Ranging slots used for different tracking architectures depending on the number of targets (mode SRq SRp NDA)	39
Figure 33. Update process scheme for Distributed MRq SRp DA depending on the number of anchors	40
Figure 34. Update process scheme for Mobile MRq SRp DA depending on the number of anchors...	40
Figure 35: Average error for different tracking architectures depending on the number of anchors for location (mode MRq SRp DA)	40
Figure 36: Number of slots per update for different tracking architectures depending on the number of anchors for location (mode MRq SRp DA)	41
Figure 37: Data slots available for communication for different tracking architectures depending on the number of anchors for location (mode MRq SRp DA).....	41
Figure 38. Update process scheme for Distributed MRq SRp DA depending on the number of targets	42
Figure 39. Update process scheme for Mobile MRq SRp DA depending on the number of targets.....	42
Figure 40: Average error for different tracking architectures depending on the number of targets (mode MRq SRp DA)	43
Figure 41: Time between updates for different tracking architectures depending on the number of targets (mode MRq SRp DA)	43
Figure 42: Data slots available for communication for different tracking architectures depending on the number of targets (mode MRq SRp DA).....	44
Figure 43: Ranging slots used for different tracking architectures depending on the number of targets (mode MRq SRp DA).....	44
Figure 44: Illustration of different routing strategies: (a) random, (b) closest and (c) furthest.....	51
Figure 45: Characteristic of the expected single-hop distance for (a) closest and (b) furthest hop strategy.....	54

Figure 46: Evaluation of the mean number of hops (a) different assumptions for furthest hop policy and (b) comparison analytical vs. experimental for all strategies.....	57
Figure 47: Evaluation of the probability distribution of the number of hops given a fixed distance for all hopping policy	59

List of Tables

Tab. 1 Interferer and channel parameters	14
--	----

Abbreviations

EUWB	CoExisting Short Range Radio by Advanced Ultra-WideBand Radio Technology
LT	Location Tracking
CRB	Cramer-Rao Bound
TOA	Time of Arrival
CR	Cognitive Radio
UWB	Ultrawide Bandwidth
AWGN	Additive White Gaussian Noise
OFDM	Orthogonal Frequency Division Multiplexing
FIM	Fisher Information Matrix
SNR	Signal-to-Noise Ratio
LDR	Low Data Rate
UWB	Ultra-Wideband
GPS	Global Positioning System
UMTS	Universal Mobile Telecommunications System
WiMAX	Worldwide Interoperability for Microwave Access
PMR	Professional Mobile Radio
RRM	Radio Resource Management
MAN	Metropolitan Area Network
WAN	Wide Area Network
MANET	Mobile Ad-hoc Network
GIS	Geographical Information System
FCC	Federal Communications Commission
NLOS	Non Line-Of-Sight
QoS	Quality of Service
TDMA	Time Division Multiple Access
FDMA	Frequency Division Multiple Access
CDMA	Code Division Multiple Access
OFDMA	Orthogonal Frequency Division Multiple Access
OFDM	Orthogonal Frequency Division Multiplexing
IEEE	Institute of Electrical and Electronics Engineers
MBWA	Mobile Broadband Wireless Access
LTE	Long Term Evolution
E-UTRA	Evolved UMTS Terrestrial Radio Access
WCDMA	Wideband Code Division Multiple Access
ICI	Inter-Cell Interference
LC	Location Controller

GTS	Guaranteed Time Slot
EKF	Extended Kalman Filter
MDS	Multi-Dimensional Scaling
MR	Measurement Report
PU	Position Update
DA	Data Aggregation
PDF	Probability density function
CDF	Cumulative distribution function
PPP	Point Poisson Process

1 Executive summary

This document is part of EUWB project addressing future UWB communication and application technologies.

The first contribution is related to the localization of unknown target (or equivalently interferers) within the Wireless Networks. Since the presence of unknown units can affect the performances and the functions of the wireless network, it is important to localize these object even if their nature is unknown.

In the following an RSSI-based localization algorithm for unknown target (whose transmitted power is unknown as the type of emitted signal) is proposed, and performances are evaluated via-matlab simulations.

This second contribution deals with the evaluation of EUWB LDR-LT platforms for simultaneous communication and tracking applications in wide indoors scenarios, which is related to the “UWB in Heterogeneous Networks” cluster. One of the main constrains of this kind of application is the availability of resources, as some resources (timeslots) will be associated to the tracking functionality, thus reducing the communication capacity. A preliminary evaluation of different system architectures and acquisition & distribution strategies in terms of resources associated to the tracking functionality was done within Task 4.2 and included in [9], although neither MAC layer timing nor resource constraints were considered. Here a complete evaluation of a simultaneous communication & tracking system based on EUWB LDR-LT platforms, including the assessment of MAC layer effect in both positioning accuracy and system capacity, is presented. Most of the system description in [9] is collected here as well in order to provide a complete view of the system.

The third contribution is the derivation of upper bounds on the multihop distributions of distances from a source to a destination N hops away yielding closed-form expressions for the average number of hops required to reach the given destination under different routing policies. Furthermore, it is presented a simple method to estimate the probability distribution $P(N|D)$ of the number of hops given a certain Euclidean distance for each hopping strategy by using the results of the average number of hops.

The results are useful to quantify the impact of hopping strategies on the performance and efficiency of multi-hop networks as well as to analyze the reliability in terms of delay and accuracy of certain applications such as flooding and localization.

2 Impact of Location Information on Communication

2.1 RSSI-based Localization of Unknown Targets/Interferers

One very frequent and common problem in many wireless systems is the presence of interferer units disturbing, or causing major troubles, to the whole network. It is therefore important that the network is able to locate the interferer units and eventually to determine its nature, in order to mitigate the effects.

In some cases these interferers can be localized and tracked like “normal” units within the network, given that localization and tracking capabilities are nowadays easily available. This happens in particular if the nature of the interferers is already known, so that also the type of the emitted signal is known by the network and the best algorithm, with the proper parameters, is used to perform localization and tracking.

If the nature of the interferers is not known, everything becomes more complex. Trying to perform localization without the proper parameters, like the signal power at the transmitter/interferer P_r or the channel model, can lead to not negligible errors.

This section provides a solution to perform localization of interferers in a very general framework, exploiting the Received Signal Strength Indicator (RSSI), i.e. the power at the receivers, without any assumption on the power emitted by the interferers.

2.1.1 Scenario Description

In the following it will be described the scenario of only one interferer. This can be done without losing generality since it is assumed that in a scenario with 2 or more interferers, they are communicating using different time-slots or bandwidth, so their signal can be distinguished by the receivers.

Define \mathbf{x}_T the location of the interferer (or, equivalently, *target* in the following) and

$$\mathbf{A} \triangleq [\mathbf{a}_1, \dots, \mathbf{a}_{n_A}] \tag{1}$$

the matrix of the *anchor nodes*, i.e. the location of the receivers of the networks.

The Euclidean distance between the interferer at \mathbf{x}_T and the generic i -th anchor at \mathbf{a}_i is defined as:

$$d_i \triangleq \|\mathbf{x}_T - \mathbf{a}_i\| = \sqrt{\langle \mathbf{x}_T - \mathbf{a}_i, \mathbf{x}_T - \mathbf{a}_i \rangle}. \tag{2}$$

The only mandatory assumption is that the target is within the *Convex Hull* $\Omega(\mathbf{A})$ defined by \mathbf{A} .

2.1.2 Model Description

2.1.2.1 WiFi Channel Model

We employ the channel model defined by ITU. The path-loss L (log-scale) is proportional to the frequency f_c , the distance d between transmitter and receiver, and is affected by shadowing (Eq. 4).

$$L(\text{dB}) = 20 \log 10 f_c + 10\alpha \log_{10} d - 28 + X \quad (3)$$

$$X \sim \mathcal{N}(0, \sigma^2) \quad (4)$$

From Eq. 3 it is possible to determine the power P_r received by the WiFi receivers, given that the transmitter is using an unknown power P_t . In the log-scale $\text{Pr}(\text{dB}) = \text{Pt}(\text{dB}) - L(\text{dB})$ and, back to the linear-scale, it is possible to write:

$$P_r = \frac{P_t}{10^{-2.8} f_c d^\alpha} s \quad (5)$$

$$s = 10^{X/10} \quad (6)$$

The path-loss factor α is a very important parameter for channel characterization: in the WiFi case it can be assumed equal to 3.

2.1.2.2 Locating the Interferer

In this subsection we will provide the mathematical model to localize the interferer with only 3 anchor nodes, i.e. the minimum necessary to perform position estimation in a 2D scenario. It is however possible to extend the model to cases with 4 or more anchor nodes.

Without loss of generality assume that $d_1 > d_2 > d_3$, i.e. that the anchor node at \mathbf{a}_1 is the farthest respect to the interferer \mathbf{x}_T and those in \mathbf{a}_3 is the nearest.

With this assumption we can define two coefficients a and b , so that d_2 and d_3 can be expressed as function of d_1 :

$$\begin{cases} \|x_T - a_1\| = d_1 \\ \|x_T - a_2\| = d_2 = \frac{1}{a} d_1 \\ \|x_T - a_3\| = d_3 = \frac{1}{b} d_1. \end{cases} \quad (7)$$

It is not possible to rewrite Eq. 7 without the first row, as in Eq. 8:

$$\begin{cases} \|x_T - a_2\| = \frac{1}{a} \|x_T - a_1\| \\ \|x_T - a_3\| = \frac{1}{b} \|x_T - a_1\|. \end{cases}$$

(8)

Given these two ratios is possible to determine the position x_T of the interferer, via a simply optimization as:

$$x_T = \underset{\Omega(A)}{\operatorname{argmin}} \left\{ \left| \|x_T - a_2\| - \frac{1}{a} \|x_T - a_1\| \right| + \left| \|x_T - a_3\| - \frac{1}{b} \|x_T - a_1\| \right| \right\}$$

(9)

The coordinates of x_T are searched within the Convex Hull $\Omega(A)$: this condition assure that there is only one acceptable solution. It is very important to remark that, since we are performing the optimization using ratios on distances and not the true Euclidean distances, the corresponding cost function has not a single minimum. There can be many combination of distances that satisfy the ratios used in the optimization: on the contrary only one set is acceptable assuming the target within the convex hull.

Here is the main idea of this work. Now the problem is not anymore how to locate the interferer (i.e. how to determine the set of three distances), but how to determine the two coefficients a and b . The network does not know the power emitted by the transmitter but only the RSSI which, from Eq. 5, is proportional to the distance (with the only exception due to the presence of bias, not considered here). The ratio between the RSSI is the same between the real distances (target-to-anchors) and, as stated in Eq. 9, is possible to estimate the target position.

Recalling Eq. 7 we have

$$\begin{cases} d_2 = \frac{1}{a} d_1 \\ d_3 = \frac{1}{b} d_1. \end{cases}$$

(10)

and therefore:

$$\begin{cases} a = \frac{d_1}{d_2} \\ b = \frac{d_1}{d_3}. \end{cases}$$

(11)

Next step is to determine the link between the distances and the RSSI P_r . We can determine the generic RSSI received by the i -th anchor in absence of noise

$$P_{r_i} = \frac{P_t}{10^{-2.8} f_c d_i^\alpha} \quad (12)$$

As it is possible to observe, there are some constant terms in the previous equation:

$$\frac{P_t}{10^{-2.8} f_c} = K \quad (13)$$

Eq. 12 can be rewritten explicating the proportionality with the distance:

$$P_{r_i} = \frac{K}{d_i^\alpha} \quad (14)$$

and

$$d_i = \sqrt[\alpha]{K/P_{r_i}} \quad (15)$$

Finally, it is possible to obtain the coefficient as the ratio between the distances:

$$\begin{cases} \frac{d_1}{d_2} = \sqrt[\alpha]{P_{r_2}/P_{r_1}} \\ \frac{d_1}{d_3} = \sqrt[\alpha]{P_{r_3}/P_{r_1}}. \end{cases} \quad (16)$$

In absence of shadowing, this model would be able to localize any interferer within the convex hull $\Omega(A)$, no matters the value of P_t . In the reality, the presence of shadowing s introduces an error while determining the coefficients a and b , causing an error on interferer position estimate.

The only unknown parameter in Eq. 16 is α , i.e. the path-loss factor, that should be estimated a-priori. In the next section, Simulation results, we will analyze the impact of the choice of this parameter.

2.1.3 Simulation results

In this section we will simulate the presence of a WiFi interferer within a network with 4 anchor nodes, disposed in the corners of a 10x10 meters square.

We have used the parameters in Tab. 1 to simulate the RSSI at each anchor nodes. Then the model described in the previous subsection has been employed to estimate the interferer position.

Variable	Value
Interferer Type	WiFi IEEE 802.11
Number of Anchor Nodes	4
Scenario Dimension	10x10 m
Interferer Location	(3,2)
f_c	2.4 GHz
P_t	-10dBW
α	3
σ	from 1 to 3

Tab. 1 Interferer and channel parameters

In Figure 1, the 4 anchor nodes, the interferer position (white square) and the different position estimations for different values of path-loss factor are depicted, with shadowing standard deviation equal to 1.

In the same figure is depicted the contour plot of the cost function described in Eq. 9 (coefficient computed assuming $\alpha=3$). Even considering the shadowing, this cost function has its minimum in correspondence of the real position of the target/interferer. This fact proves the robustness of the optimization model.

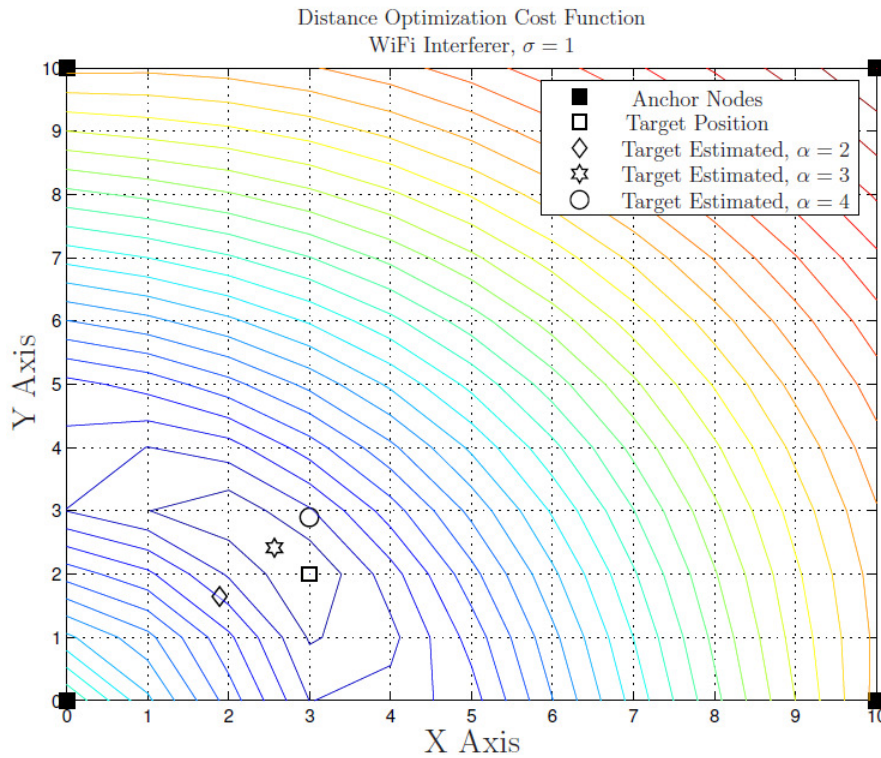


Figure 1: Target position estimation for different value of path-loss factor.

It is interesting to note that, if the proper path-loss function is employed in the optimization, the position estimation of the target is almost correct, with a minimum error. In this case $\alpha=3$; with different values of path-loss factor there is a growing localization error.

The impact of the correct choice of path loss is depicted in Figure 2. Three curves are plotted, for different values of noise variance. The impact of shadowing is secondary respect to the choice of the correct path-loss factor.

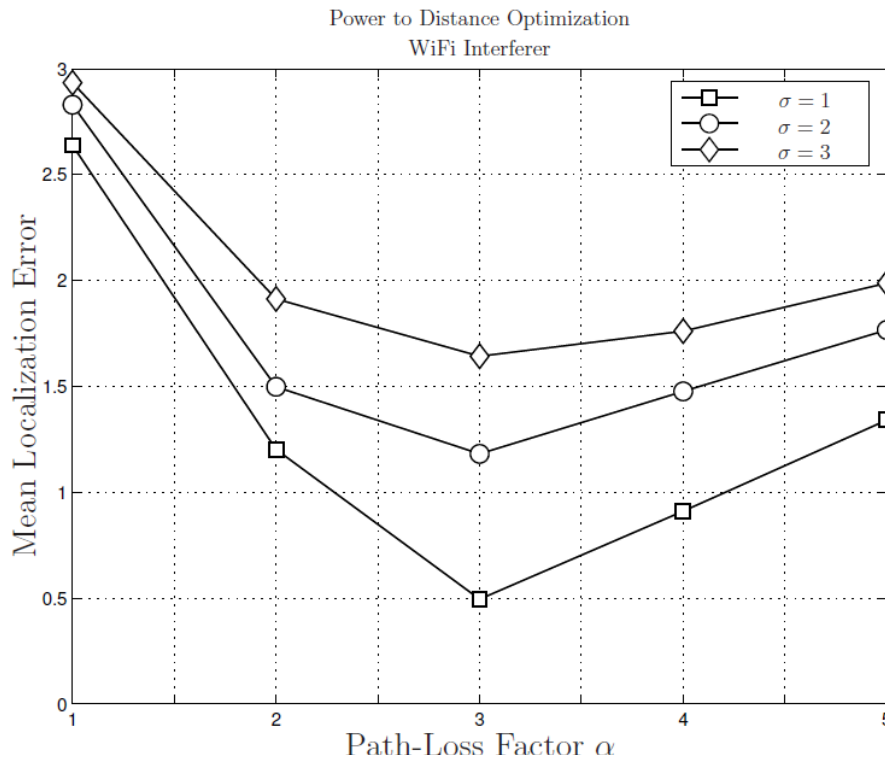


Figure 2: Target Localization Error (in meters) for different value of path-loss factor and different shadowing levels

A wrong choice of α can lead to a big localization error; on the contrary with the right path-loss factor, it is possible to obtain a good precision.

These results show that the only real challenge in this case is to choose the right path-loss factor in order to obtain good interferer localization results.

2.1.4 Future Research Directions

The first results of this work have proved to be very promising and very easy to be implemented. The possibility to localize the interferers without knowing the type of emitted signal and the power emitted, can represent a big improvement for network performances.

The main issue still open is related to α . It is desirable to choose the path-loss factor in a more rigorous and robust way. For this reason, can be chosen 2 or 3 more likely path-loss factor and then to determine which one seems to best match the received signal.

This technique will be employed within WP3 to obtain a radio map of the interferers. Finally the model will be evaluated through on-field measurement and not only via-matlab simulation.

2.1.5 Conclusion

The RSSI-based optimization technique for unknown targets has proved to be a robust model to perform localization of interferers or object whose nature is unknown, only exploiting the RSSI. The only open issue is related to the path-loss factor, whose partially related to the scenario in which the target is present and partially to the nature of the target itself. A possible research direction is the developing of an appropriate tuning-phase of the system, through some preliminary evaluations of the scenario, in order to develop an algorithm to choose the best-fitting parameter.

2.2 Analysis of Combined Communication and Tracking Systems

This section deals with the evaluation of EUWB LDR-LT platforms for simultaneous communication and tracking applications in wide indoors scenarios, which is related to the “UWB in Heterogeneous Networks” cluster. One of the main constrains of this kind of application is the availability of resources, as some resources (timeslots) will be associated to the tracking functionality, thus reducing the communication capacity. A preliminary evaluation of different system architectures and acquisition & distribution strategies in terms of resources associated to the tracking functionality was done within Task 4.2 and included in [9], although neither MAC layer timing nor resource constraints were considered. Here a complete evaluation of a simultaneous communication & tracking system based on EUWB LDR-LT platforms, including the assessment of MAC layer effect in both positioning accuracy and system capacity, is presented. Most of the system description in [9] is collected here as well in order to provide a complete view of the system.

2.2.1 Introduction

Due to its great accuracy and good performance on multipath and NLOS environments, UWB is good candidate to provide location information to mobile users in indoor environments. Some interesting scenarios include shopping malls, train stations, airports, exhibition centres, sports stadiums, etc. This would enable the development of location based services (LBS). Indoor positioning systems, location-aware search or proximity marketing are among the possible applications of location based services. For example, a user in a shopping centre would be able to position himself in a map on his mobile just like a car navigation system and ask for the route to a certain shop, search for the closest restaurant and receive information of the closest shops such as latest bargains or special discounts.

Several UWB-based indoor LT systems can already be found in the market. Nevertheless, all these systems are proprietary solutions not compliant with any standard. Furthermore, they do not provide simultaneous communication and localization. Sensors/receivers are connected with the location engine via Ethernet, while tags do not have any communication capability and do not provide any kind of interface for integration with a device. In contrast to proprietary solutions, solutions based on a standard, i.e. 802.15.4a, would allow interoperability between different existing solutions and facilitate integration into user's devices, e.g. a mobile phone or PDA with an 802.15.4a interface would be able to communicate with any 802.15.4a peripheral and to retrieve its position from an 802.15.4a LT system.

Thanks to the simultaneous data transmission and location capabilities of UWB, a single UWB network could be used to interconnect different sensors (e.g. fire detection sensors) and to track mobile users. This characteristic is very important in order to minimize the fixed infrastructure, as one single network would provide both functionalities, and cabling, as sensors would be wirelessly

connected. Furthermore, users would be able to access information of interest through UWB besides retrieving their position.

Nevertheless, the application of the UWB technology for the development of combined data transmission and location networks in relatively wide indoor scenarios has to face important challenges due to the short range of UWB and the limited data rate of LDR-LT (Low Data Rate with Location and Tracking) UWB systems.

First of all, the area of interest can be relatively large (length over hundreds of meters) in relation to UWB range (10-50 meters), which implies that the area of interest will be covered by a high number of anchor nodes (fixed reference nodes with known positions) and eventually different UWB picocells. System architecture and network topology must be carefully selected in order to deal with the large size of the network.

Any localization system based on TOA estimation entails the exchange of ranging frames between the anchor nodes and the target nodes (mobile nodes to be tracked). Furthermore, estimated distances must be transmitted to a location controller (LC) that computes target's position. This means that some temporal resources (timeslots) must be dedicated to localization with the consequent reduction of the available data rate for non-localization data communication. The mobility of users implies that position update rate must be relatively high in order to keep the error of the estimated position under a reasonable value. But a higher update rate entails a higher need of resources. Finally, the system should be able to cope with a high number of users, which entails an increase of the resources needed for location. Therefore, the amount of resources that are needed for the tracking application must be carefully evaluated in order to guarantee that the system can cope with the required accuracy and number of users and on the other hand provide a suitable data rate for communication with a reasonable complexity level.

2.2.2 System description

2.2.2.1 MAC layer description

In order to evaluate the amount of resources and the traffic load associated with the tracking application, we have considered real MAC & PHY layers developed within EUWB project. Superframe structure defines the temporization of slots used for each purpose (neighbour discovery, communication, ranging...). On the other hand, network topology impacts on how data packets containing location information are transmitted/relayed between the different nodes.

EUWB MAC layer has been designed for Low Data Rate, Location and Tracking (LDR-LT) applications. It is based on IEEE 802.15.4 standard [10], with enhancements to meet quality of service requirements and to provide efficient support for ranging and localization with an ultra-wide-band (UWB) physical layer. A detailed description of EUWB MAC layer can be found in [11].

A MAC superframe structure is defined, which is divided into timeslots where the different frames (beacon frames, hello frames, data frames, ranging frames, timeslot requests...) are sent. Superframe structure is shown in Figure 3. Two main periods are defined in the superframe, namely Control period and Data period. In the "Control period", two parts are identified:

- The Beacon period used for the beacon alignment
- The Topology Management period used to send the "Hello" frames

The other portion called “Data Period” is used for data frames, ranging frames, GTS request frames and other command frames. Data Frames, ranging frames and GTS request frames are sent in a Contention Free Period whereas other command frames are sent in the Contention Access Period (CAP). Ranging slots are considered as data slots and ranging frames are sent in the CFP period as other data frames.

The Contention Free Period in the “Data Period” is so composed of:

- Guaranteed time slots (GTS) for data frame transfer, acknowledgments and ranging. The number of GTS used for ranging can be freely defined. It depends of the number of devices which are requested to perform ranging as well as the number of ranging measurements needed for a localisation update.
- A GTS request period used to send the GTS request frames.

The maximum number of slots (and so sub-slots) for each part of the frame are then the following ones:

- 12 Timeslots in the Beacon period
- 3 Timeslots in the Topology Management Period (12 sub-slots as each slot is divided in 4 sub-slots)
- 20 Timeslots in the GTS Period that are used for Data communications and for ranging as the ranging slots are considered as data slots. A classical case will be to have 8 Timeslots for data communication and 12 Timeslots for ranging enabling 4 devices using 3-way ranging.
- 6 Timeslots in the GTS request Period
- 12 Timeslots in the CAP period

So, the maximum number of slots in the superframe is 53. If the maximum number of slots is not achieved in the superframe, an inactive part is defined before the beginning of the next superframe.

BP: Beacon Period
 TP: Topology Management Period
 IP: Inactive Period

CFP: Contention Free Period
 CAP: Contention Access Period

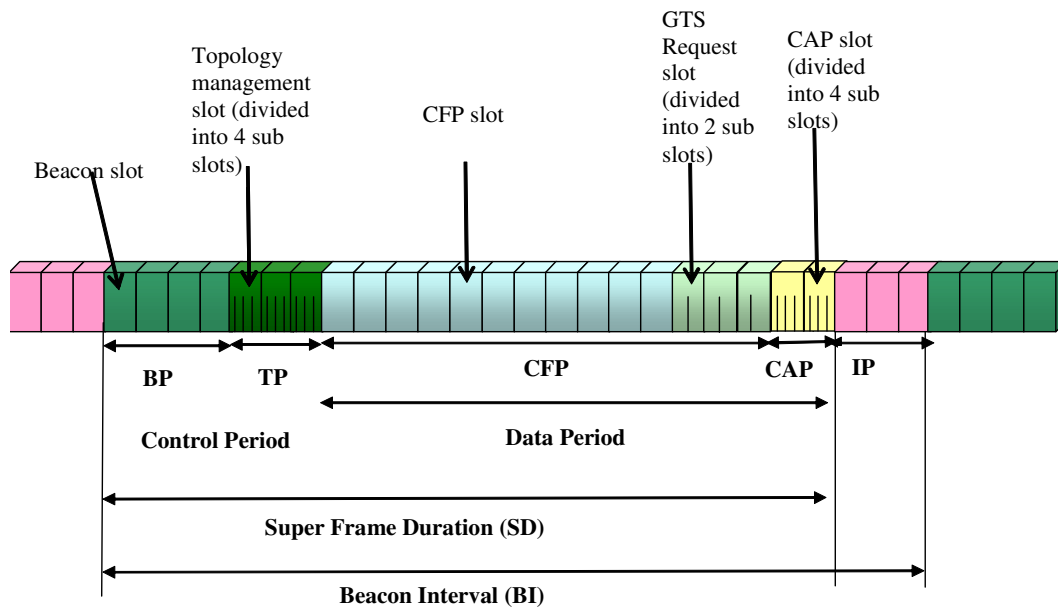


Figure 3: EUWB MAC superframe structure [11]

Concerning network topology, the piconet is the basic unit. Piconets are based in a mesh centralized topology, which is defined by a centralised allocation management and a centralised common timing reference synchronisation. Indeed a coordinator is elected in the network so as to transmit beacon frames and to handle the scheduling procedures.

Figure 4 describes the construction of a Mesh centralised network. First a scheduling tree is built, which is used to transport beacon, association request and GTS request command frames. Then it is extended to a meshed scheduling tree by enabling the transmission out of the tree for the data. Data frames, ranging frames can so be sent out of the tree as well as hello frames that are broadcasted to the neighbours. The CFP slots for each link are allocated by the piconet coordinator for the whole route between the source and the destination.

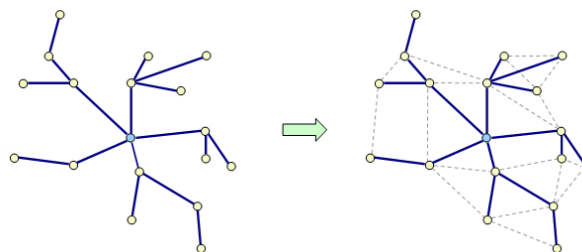


Figure 4: Mesh centralized topology [11]

In the scheduling tree, the Piconet Coordinator is on top of the tree. Then the different devices are defined by their scheduling tree level. The typical maximum tree level that must be taken into account for the application scenario is 4. Then a possible scheduling tree can be represented as follows.

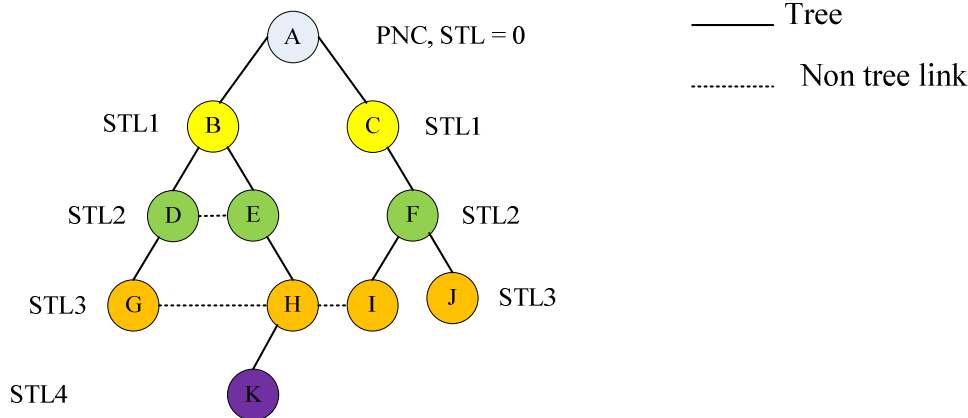


Figure 5: Example of meshed scheduling tree [11]

The scheduling tree is used to transport the beacon frames to each device of the network. It allows also the transmission of the GTS request frames from the devices to the coordinator, the association request frames and the disassociation request frames.

Data frames, hello frames, ack frames and ranging frames can be sent on non tree link. Hello frames are broadcasted and so no destination address is needed. Ranging frames are not relayed and can be sent only between neighbours. The neighbourhood is known locally for each node of the network thanks to the hello frames that are periodically sent.

It is to be noticed also that the relaying procedure is performed at the MAC layer level. The source node requests an allocation to the coordinator for the entire route. Indeed, when a node has data to transmit, it will send a GTS request on the tree to the coordinator with its address as the source address and the destination address of the transmission. The request will correspond to the number of GTS slots needed for the data transmission on a link. The coordinator which has the knowledge of the whole network will look on its routing table if there are relays between the source and the destination. If there are relays, the coordinator will allocate the GTS for each link based on the request made by the source node. The GTS allocation will be available to the source node and relay nodes in the Beacon frame (Data descriptor in the GTS fields).

2.2.2.2 *LT system description*

The objective of the LT system is to track the position of mobile users in relatively wide indoor environments. With that purpose a UWB simultaneous data transmission and location network will be deployed on the scenario. The network is composed of N_a anchors, fixed and regularly distributed at known positions, and N_m targets, mobile nodes to be located.

In order to track the position of the target nodes, location information, basically the distances estimated between the target and anchor nodes, must be acquired and transmitted to the location controllers, which are the functional units that execute the tracking algorithm to obtain the estimated position of the targets. Location controllers can be physically implemented in one or more anchor nodes or in the mobile nodes, depending on the architecture which is defined.

Tracking may be performed with all the anchors in coverage of a given target or with a subset of them. If ranging is performed with a subset of the neighbour anchors, then a selection procedure must be defined in order to select the closest anchors. This procedure must be based in the available

information such as previously estimated distances, estimated position of the target, position of the anchors, power measurements, etc.

The acquisition of the location information is done through the ranging procedure. Three procedures are defined [12]

- One way ranging: The target node transmits a ranging packet and every anchor measures the time of arrival of the ranging packet. The position of the target can be obtained from the differences between the times of arrival on each anchor. Only one time slot is needed but it requires synchronization between all the anchors.
- Two way ranging: The procedure initiator (target or anchor) transmits a ranging request to another node, which estimates the time of arrival and sends a ranging response after a predefined time. The initiator measures the time of arrival of the response and can estimate the transmission delay and the distance between the nodes. Two time slots are needed, but there is no need of synchronization between the nodes.
- Three way ranging: Similar to the two way ranging scheme, but in this case two ranging responses are sent in order to compensate the clock drift. The ranging procedure can be initiated by the target nodes or by the anchor nodes and the distance is estimated by the initiator. It requires three time slots, but estimated distances are much more accurate.

Once the distances between the target and the anchor nodes are estimated, they must be transmitted to the location controller in a data packet (measurement report data packet). The location controller executes the tracking algorithm to calculate the position and transmits the updated position to the target node (position update data packet).

In order to reduce the amount of resources needed to acquire and distribute the location information, different enhanced modes are proposed and explained in detail in [13]. These enhancements include:

- Data aggregation: All the distances estimated can be aggregated and sent by the ranging initiator (target or anchor) in a single measurement report data packet to the LC.
- Broadcast/multicast request: In order to reduce the number of slots, in case ranging is initiated by targets, a target can aggregate multiple ranging requests into a single ranging request sent to all its neighbour anchors (target broadcast request) or to a set of anchors (target multicast request). In case ranging is initiated by anchors, an anchor can aggregate multiple ranging requests into a single ranging request sent to all its neighbour targets (anchor broadcast request) or to a set of targets (anchor multicast request).
- Multicast response: In case ranging is initiated by targets and after receiving the ranging requests from different targets, an anchor can aggregate the responses to the involved targets into a single ranging response (anchor multicast response). In case ranging is initiated by anchors and after receiving the ranging requests from different anchors, a target can aggregate the responses to the involved anchors into a single ranging response (target multicast response).

If the initiator is the target node, anchor multicast response would require a simultaneous update of the position of all the targets in order to be able to aggregate the responses to multiple targets into a multicast response packet. The same applies for anchor broadcast/multicast request when the initiator is the anchor node, as the anchor must aggregate the requests to multiple targets into a multicast request packet. Finally, it also applies to data aggregation when the initiator is the anchor node, as the anchor must aggregate distances estimated to multiple targets into a single measurement report data packet sent to the LC.

2.2.2.3 Tracking Function Distribution in the Network

The tracking functionality is executed by the LCs, which can be physically located in one or more anchor nodes or in the target nodes. Depending on the location of the LC, several architectures (centralized and distributed) can be defined.

If a centralized in the network architecture is assumed, the tracking functionality is implemented in one or more previously defined anchor nodes that become LCs. Using one LC entails a higher need of resources, as multiple hops will be needed to forward the location information to the LC. Defining multiple LCs reduces the need of resources, but increases complexity, as the tracking functionality must be implemented in several nodes and a procedure should be implemented to assign each target to the closest LC.

In the distributed architecture, each target picks dynamically one of its neighbour anchors to execute the tracking functionality. Therefore, there may be as many simultaneous LCs as targets. As the LC is always executed by an anchor neighbour to the target, only one timeslot will be needed to exchange data frames between the target and the LC, and resources will consequently be reduced. As a drawback, the tracking functionality must be implemented in every anchor.

Finally, in the architecture centralized in the mobile nodes the LC function is implemented in the target nodes. The target nodes perform ranging with their neighbour anchors and obtain their own position applying the tracking algorithm. Therefore, there is no need of transmitting the estimated distances and the updated position. Nevertheless, the feasibility of this architecture depends on the computational capability of the devices to be tracked.

2.2.2.4 Simulator description

In order to evaluate different system architectures, tracking algorithms, and the impact of the different system design parameters, a simulation tool has been developed, using C++ as programming language and Visual Studio .NET as development platform.

The simulator scenario is the representation of a relatively wide indoors area of dimensions *length* x *width*. On this scenario a UWB network is deployed, as it is shown in Figure 6. The network is composed of N_a anchors, fixed and regularly distributed at known positions, and N_m targets, mobile nodes to be located. For simplicity, the scenario is covered by a single UWB piconet, so data transmission between different piconets and handover are not further considered.

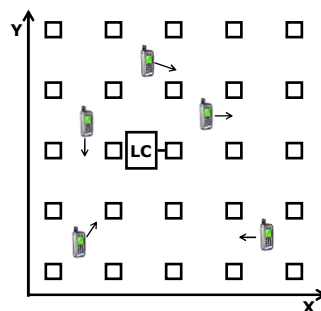


Figure 6: UWB location simulator scenario

The dynamics of the mobile nodes are modelled by random directions and speeds that are constant during a certain period of time, after which new random directions and speeds are set. The dynamic model is characterized by maximum and minimum speeds and the direction change rate.

In order to track the position of the target nodes, the distances between the target and anchor nodes are estimated (ranging). Ranging may be performed with all the anchors in coverage of a given target or with a subset of them. A ranging model is used to characterize the ranging error distribution and to generate distance estimation samples. Estimated distances are sent to location controllers, which are the functional units that execute the tracking algorithm to obtain the estimated position of the targets. Location controllers can be physically implemented in one or more anchor nodes or in the mobile nodes, depending on the architecture which is defined. Finally, the estimated positions are sent to each target.

2.2.2.5 Ranging model

The acquisition of the location information, i.e. distances between the anchor nodes and target nodes, is done through the ranging procedure. A ranging model is used to characterize the ranging error distribution and to generate distance estimation samples. The ranging model that has been implemented was proposed within PULSERS PHASE II [13] and the specific model and parameters used can be found in [14][15].

Range measurements based on round-trip Time of Flight (ToF) estimation through n-Way Ranging transactions can be modelled as:

$$\tilde{d}_{ij} = d_{ij} + \varepsilon_{ij} + n_{ij} = d'_{ij} + n_{ij}$$

Eq. 1: Range measurement model

where d_{ij} is the actual distance between nodes i and j , d'_{ij} is the biased distance (with bias ε_{ij}) and n_{ij} is a residual noise term.

The biased distance is modelled as a weighted sum of Gaussian and Exponential components conditioned upon the actual distance and the channel configuration (LOS/NLOS/NLOS2), as proposed in [14]. The pdf of d' , conditioned upon d and a particular channel configuration C , is then described as follows:

$$p_c \left[d' / (d, C) \right] = G_c \frac{1}{d} \frac{1}{\sqrt{2\pi}\sigma_c} e^{-\frac{\left(\frac{d'}{d}-1\right)^2}{2\sigma_c^2}} + E_c \frac{1_{\{d'>d\}}}{d} \lambda_c e^{-\lambda_c \left(\frac{d'}{d}-1\right)}$$

Eq. 2: Conditional pdf of biased distances in the "Mixed bias" model

where $d \neq 0$, $\{G_c, \sigma_c\}$ and $\{E_c, \lambda_c\}$ are the weights and parameters of Gaussian and Exponential mixture components, $1_{\{x>y\}} = 1$ whenever $x>y$ and 0 otherwise, and C takes its value among $\{LOS, NLOS, NLOS2\}$.

The residual noise is modelled as additive and centred, with a variance σ_n^2 that depends on detection noise terms affecting unitary ToA estimates and involved protocol durations.

Finally, the model was enhanced by taking into account the probability $W_C(d)$ to have a particular channel configuration at d . As a result of the indoor measurement campaign in [14], these weights have been described as Gaussian-like functions:

$$W_C(d) = \frac{\xi}{\sqrt{2\pi}\zeta_C} e^{-\frac{(d-d_C)^2}{2\zeta_C^2}}$$

Eq. 3: Probabilities of channel configurations as continuous Gaussian-like functions

2.2.2.6 Tracking algorithms

With respect to the tracking technique itself, parametric and non-parametric approaches can be distinguished. Parametric approaches compute the location based on the a priori knowledge of a model, while non-parametric approaches process straightforward the data with the usage, in some cases, only of some statistic parameters (mean, variance). Specifically, the following algorithms are implemented in the simulator:

- Trilateration

Trilateration is a non-parametric algorithm that computes the position based on the distance estimated between the target and three anchor nodes using a geometrical method for determining the intersection of three sphere surfaces. Consequently, only three anchors are used for position computation. If a higher number of anchors are selected, then the three with smallest estimated distance to the target are used.

- Extended Kalman filter (EKF)

EKF is a Bayesian technique known for its low-complexity, performance and stability as a tracking algorithm [16]. The Kalman-based tracking algorithm has two major stages, namely, the update and the correction stages, which are iterated k times for every observation occurring at a given time. With this purpose, function f that describes the evolution of the state vector through time, and function h that describes the relation between the state vector and the measure vector, must be characterised. For the implementation of the filter, we have taken advantage of `kfilter`, which is a C++ variable-dimension extended Kalman filter free software library under a GNU license [17]. In order to ensure a fast convergence from the beginning, the first position is computed using trilateration and this position is used to initialize the filter.

- Multidimensional scaling

Multidimensional scaling (MDS) is a multivariate data analysis technique used to map “proximities” into a space [18]. Given n points and corresponding dissimilarity, MDS finds a set of points in a space such that a one-to-one mapping between the original configuration and the reconstructed one exists. Then it is possible to map back the solution to the absolute reference system used by Procrustes transformation. The implementation of Multidimensional Scaling has been based on the implementation done at the EUWB platforms (PULSERS 2 approach) [19]. In fact, this implementation is not a classic MDS solution, but a combination of MDS with a weighted least squares minimization (WLS). MDS is used to obtain a previous estimation of the solution. Then, a low-complexity algorithm based on majorization technique is applied, known as SMACOF. Nevertheless, the simulator implementation does not take into account weights, as successive ranging estimations are uncorrelated. The advantage of a non parametric approach is its ability to exploit the data remaining completely model independent.

- Particle filter

An interesting alternative to the classical approach are recursive implementations of Monte Carlo based statistical signal processing, which are known as particle filters [20]. Particle filters allow using non-Gaussian noise and non-linear models, although their computational complexity is higher. The particle filter is based on a high number of samples of the state vector or particles, which are weighted according to their importance (likelihood) in order to provide an estimation of the state vector. On each step, the particles are moved according to the dynamic model and the weights are updated according to the likelihood of the observations (estimated distances) using a measurement error model.

For the implementation of the particle filter, we have taken advantage of SMCTC, a C++ template class library for the implementation general Sequential Monte Carlo algorithms, which is provided under a GNU license [21]. In order to ensure a fast convergence from the beginning, the first position is computed using trilateration and this position is used to initialize the particles.

2.2.3 Analysis and evaluation

The system performance has been evaluated in terms of positioning error (average, variance, root mean square error, error distribution...) and the amount of resources used for location (number of time slots).

With this purpose, several simulations have been performed for the different proposed architectures and acquisition and dissemination of location information strategies. The influence of other design parameters has also been analyzed.

For these simulations, a common set of parameters has been defined. Simulation duration has been set to 10000 seconds. The area size has been set to 50 m. x 50 m. By default, the area is covered by 36 anchors uniformly distributed with a distance between anchors to 10 m., 1 target is tracked and 4 anchors are used to position each target, although these parameters are varied through the simulations. Concerning the dynamics of the mobile nodes, minimum and maximum speeds have been set to 0.1 and 3 m/s respectively, and direction changes every 20 seconds. Position update rate has been set to 976 ms (5 superframes) and UWB nodes range to 15 m. Three way ranging has been considered and trilateration has been used as tracking algorithm.

2.2.3.1 Data acquisition & distribution enhancements

The amount of resources needed for location have been simulated for each enhancement based on an architecture centralized in the network with one location controller (1LC), one mobile target and a distance between anchors of 10 meters, which results into 36 anchors. The number of anchors used for positioning the target is variable. For the data acquisition & distribution enhancements, which were described in detail in Section 2.2.2.2, the following notation has been used:

- SRq: Single request
- MRq: Multicast request
- SRp: Single response
- MRp: Multicast response
- NDA: No data aggregation
- DA: Data aggregation

In order to analyse the results, it is necessary to understand how the position update process is carried out for each one of the enhancements. With this purpose, Figure 7 shows a scheme of the update process for the architecture centralized in the network with 1 LC, single request, single response and no data aggregation, depending on the number of anchors used for positioning. Each row represents the GTS period of a superframe, which is used for ranging exchanges and data transmission. GTS period duration is 20 slots, with 12 slots allocated to ranging and 8 slots to data transmission. Concerning the frames sent on each slot, the following notation has been used:

- Rq_{ij}: Ranging request from target i to anchor j

- Rq_i : Multicast ranging request from target i
- Rp_{ij} : Ranging response from anchor j to target i
- Rp_j : Multicast ranging response from anchor j
- MR_{ij} : Measurement report data frame containing distance between target i and anchor j
- MR_i : Aggregated measurement report data frame containing distances estimated by target i
- PU_i : Position update data frame for target i

As Three-Way ranging is used, two ranging responses are generated for each ranging request. As the architecture is centralized in the network with 1 LC, in general multiple hops will be needed to relay the data frames from the target to the LC and vice versa. Consequently, in the scheme MR and PU frames use 2 slots, as it has been identified that for this configuration (36 anchors and 1 LC) the average number of hops between the target and the LC is approximately 1.9, although it varies between 1 and 3 slots depending on the distance between the target and the LC.

3 anchors	Rq_{i1}	Rp_{i1}	Rp_{i1}	Rq_{i2}	Rp_{i2}	Rp_{i2}	Rq_{i3}	Rp_{i3}	Rp_{i3}					MR_{i1}	MR_{i1}	MR_{i2}	MR_{i2}	MR_{i3}	MR_{i3}	PU_i	PU_i	
4 anchors	Rq_{i1}	Rp_{i1}	Rp_{i1}	Rq_{i2}	Rp_{i2}	Rp_{i2}	Rq_{i3}	Rp_{i3}	Rp_{i3}	Rq_{i4}	Rp_{i4}	Rp_{i4}	MR_{i1}	MR_{i1}	MR_{i2}	MR_{i2}	MR_{i3}	MR_{i3}	MR_{i4}	MR_{i4}		
													PU_i	PU_i								
5 anchors	Rq_{i1}	Rp_{i1}	Rp_{i1}	Rq_{i2}	Rp_{i2}	Rp_{i2}	Rq_{i3}	Rp_{i3}	Rp_{i3}	Rq_{i4}	Rp_{i4}	Rp_{i4}	MR_{i1}	MR_{i1}	MR_{i2}	MR_{i2}	MR_{i3}	MR_{i3}	MR_{i4}	MR_{i4}		
	Rq_{i5}	Rp_{i5}	Rp_{i5}										MR_{i5}	MR_{i5}	PU_i	PU_i						
6 anchors	Rq_{i1}	Rp_{i1}	Rp_{i1}	Rq_{i2}	Rp_{i2}	Rp_{i2}	Rq_{i3}	Rp_{i3}	Rp_{i3}	Rq_{i4}	Rp_{i4}	Rp_{i4}	MR_{i1}	MR_{i1}	MR_{i2}	MR_{i2}	MR_{i3}	MR_{i3}	MR_{i4}	MR_{i4}		
	Rq_{i5}	Rp_{i5}	Rp_{i5}	Rq_{i6}	Rp_{i6}	Rp_{i6}							MR_{i5}	MR_{i5}	MR_{i6}	MR_{i6}	PU_i	PU_i				
7 anchors	Rq_{i1}	Rp_{i1}	Rp_{i1}	Rq_{i2}	Rp_{i2}	Rp_{i2}	Rq_{i3}	Rp_{i3}	Rp_{i3}	Rq_{i4}	Rp_{i4}	Rp_{i4}	MR_{i1}	MR_{i1}	MR_{i2}	MR_{i2}	MR_{i3}	MR_{i3}	MR_{i4}	MR_{i4}		
	Rq_{i5}	Rp_{i5}	Rp_{i5}	Rq_{i6}	Rp_{i6}	Rp_{i6}	Rq_{i7}	Rp_{i7}	Rp_{i7}				MR_{i5}	MR_{i5}	MR_{i6}	MR_{i6}	MR_{i7}	MR_{i7}	PU_i	PU_i		

Figure 7. Update process scheme for 1LC SRq SRp NDA depending on the number of anchors

Figure 8 shows a similar scheme when multicast request is used. Note that now only one ranging request is used on each update process.

3 anchors	Rq_i	Rp_{i1}	Rp_{i1}	Rp_{i2}	Rp_{i2}	Rp_{i3}	Rp_{i3}						MR_{i1}	MR_{i1}	MR_{i2}	MR_{i2}	MR_{i3}	MR_{i3}	PU_i	PU_i		
4 anchors	Rq_i	Rp_{i1}	Rp_{i1}	Rp_{i2}	Rp_{i2}	Rp_{i3}	Rp_{i3}	Rp_{i4}	Rp_{i4}				MR_{i1}	MR_{i1}	MR_{i2}	MR_{i2}	MR_{i3}	MR_{i3}	MR_{i4}	MR_{i4}		
													PU_i	PU_i								
5 anchors	Rq_i	Rp_{i1}	Rp_{i1}	Rp_{i2}	Rp_{i2}	Rp_{i3}	Rp_{i3}	Rp_{i4}	Rp_{i4}	Rp_{i5}	Rp_{i5}		MR_{i1}	MR_{i1}	MR_{i2}	MR_{i2}	MR_{i3}	MR_{i3}	MR_{i4}	MR_{i4}		
													MR_{i5}	MR_{i5}	PU_i	PU_i						
6 anchors	Rq_i	Rp_{i1}	Rp_{i1}	Rp_{i2}	Rp_{i2}	Rp_{i3}	Rp_{i3}	Rp_{i4}	Rp_{i4}	Rp_{i5}	Rp_{i5}		MR_{i1}	MR_{i1}	MR_{i2}	MR_{i2}	MR_{i3}	MR_{i3}	MR_{i4}	MR_{i4}		
	Rq_i	Rp_{i6}	Rp_{i6}										MR_{i5}	MR_{i5}	MR_{i6}	MR_{i6}	PU_i	PU_i				
7 anchors	Rq_i	Rp_{i1}	Rp_{i1}	Rp_{i2}	Rp_{i2}	Rp_{i3}	Rp_{i3}	Rp_{i4}	Rp_{i4}	Rp_{i5}	Rp_{i5}		MR_{i1}	MR_{i1}	MR_{i2}	MR_{i2}	MR_{i3}	MR_{i3}	MR_{i4}	MR_{i4}		
	Rq_i	Rp_{i6}	Rp_{i6}	Rq_{i7}	Rq_{i7}								MR_{i5}	MR_{i5}	MR_{i6}	MR_{i6}	MR_{i7}	MR_{i7}	PU_i	PU_i		

Figure 8. Update process scheme for 1LC MRq SRp NDA depending on the number of anchors

Figure 9 shows the update process scheme when data aggregation is applied. It must be noted that now only one measurement report is sent to the LC, although it may need multiple slots. Finally, Figure 10 shows the update process scheme when both multicast request and data aggregation are applied. Multicast request has not been considered as only one target is tracked.

3 anchors	Rq ₁₁	Rp ₁₁	Rp ₁₁	Rq ₁₂	Rp ₁₂	Rp ₁₂	Rq ₁₃	Rp ₁₃	Rp ₁₃				MR ₁	MR ₁	PU ₁	PU ₁				
4 anchors	Rq ₁₁	Rp ₁₁	Rp ₁₁	Rq ₁₂	Rp ₁₂	Rp ₁₂	Rq ₁₃	Rp ₁₃	Rp ₁₃	Rq ₁₄	Rp ₁₄	Rp ₁₄	MR ₁	MR ₁	PU ₁	PU ₁				
5 anchors	Rq ₁₁	Rp ₁₁	Rp ₁₁	Rq ₁₂	Rp ₁₂	Rp ₁₂	Rq ₁₃	Rp ₁₃	Rp ₁₃	Rq ₁₄	Rp ₁₄	Rp ₁₄								
	Rq ₁₅	Rp ₁₅	Rp ₁₅										MR ₁	MR ₁	PU ₁	PU ₁				
6 anchors	Rq ₁₁	Rp ₁₁	Rp ₁₁	Rq ₁₂	Rp ₁₂	Rp ₁₂	Rq ₁₃	Rp ₁₃	Rp ₁₃	Rq ₁₄	Rp ₁₄	Rp ₁₄								
	Rq ₁₅	Rp ₁₅	Rp ₁₅	Rq ₁₆	Rp ₁₆	Rp ₁₆							MR ₁	MR ₁	PU ₁	PU ₁				
7 anchors	Rq ₁₁	Rp ₁₁	Rp ₁₁	Rq ₁₂	Rp ₁₂	Rp ₁₂	Rq ₁₃	Rp ₁₃	Rp ₁₃	Rq ₁₄	Rp ₁₄	Rp ₁₄								
	Rq ₁₅	Rp ₁₅	Rp ₁₅	Rq ₁₆	Rp ₁₆	Rp ₁₆	Rq ₁₇	Rp ₁₇	Rp ₁₇				MR ₁	MR ₁	PU ₁	PU ₁				

Figure 9. Update process scheme for 1LC SRq SRp DA depending on the number of anchors

3 anchors	Rq ₁	Rp ₁₁	Rp ₁₁	Rp ₁₂	Rp ₁₂	Rp ₁₃	Rp ₁₃						MR ₁	MR ₁	PU ₁	PU ₁				
4 anchors	Rq ₁	Rp ₁₁	Rp ₁₁	Rp ₁₂	Rp ₁₂	Rp ₁₃	Rp ₁₃	Rp ₁₄	Rp ₁₄				MR ₁	MR ₁	PU ₁	PU ₁				
5 anchors	Rq ₁	Rp ₁₁	Rp ₁₁	Rp ₁₂	Rp ₁₂	Rp ₁₃	Rp ₁₃	Rp ₁₄	Rp ₁₄	Rp ₁₅	Rp ₁₅		MR ₁	MR ₁	PU ₁	PU ₁				
6 anchors	Rq ₁	Rp ₁₁	Rp ₁₁	Rp ₁₂	Rp ₁₂	Rp ₁₃	Rp ₁₃	Rp ₁₄	Rp ₁₄	Rp ₁₅	Rp ₁₅									
	Rq ₁	Rp ₁₆	Rp ₁₆										MR ₁	MR ₁	PU ₁	PU ₁				
7 anchors	Rq ₁	Rp ₁₁	Rp ₁₁	Rp ₁₂	Rp ₁₂	Rp ₁₃	Rp ₁₃	Rp ₁₄	Rp ₁₄	Rp ₁₅	Rp ₁₅									
	Rq ₁	Rp ₁₆	Rp ₁₆	Rq ₁₇	Rq ₁₇								MR ₁	MR ₁	PU ₁	PU ₁				

Figure 10. Update process scheme for 1LC MRq SRp DA depending on the number of anchors

Figure 11 shows the average positioning error for each one of the acquisition & distribution schemes depending on the number of anchors. Average error for an ideal case when MAC timing and constraints are not considered is included as a reference. In general, the error for the MAC simulations is always higher than the ideal case due to the latency of the position update process, in particular the number of superframes that are needed. Note that results are constant for 7 or more anchors as with this configuration (10 m between anchors) the target is not likely to be in coverage of more than 7 anchors.

Concerning the Srq SRp NDA mode, the error when 3 anchors are used is slightly higher than the ideal case, as when the target is 1 or 2 hops away from the LC the process will be carried out within a single superframe, and only when the target is 3 hops away from the LC a second superframe would be needed, thus increasing the latency and the error. When 4 anchors are used, 2 superframes would be needed also when the target is 2 hops away from the LC, so the error increases. For 5 anchors, 2 superframes are always needed in order to perform all the ranging exchanges, so the error increases. For 6 anchors there is a further increase of the error as 3 superframes would be needed when the anchor is 3 hops away from the LC. When 7 anchors are used, the need of superframes is similar to the case with 6 anchors, but in this case there are 3 recently estimated distances (in the same superframe) and 4 delayed estimated distances (in the previous superframe), whereas with 6 anchors there was 2

recently estimated distances and 4 delayed, so there is a slight decrease of the error. Results are very similar for MRq SRp NDA except when 5 anchors are used. In this case, with single request always 2 superframes were needed to perform all the ranging procedures, whereas if multicast request is used all the ranging exchanges can be carried out within a superframe, and only 1 superframe will be needed if the target is 1 hop away from the LC, so the error is similar to the case with 4 anchors.

When data aggregation is used, the limitation will be always due to the ranging exchanges, as location data exchanges will be carried out always in a single superframe. With single request (SRq SRp DA) one superframe will be needed when 3 or 4 anchors are used, and two superframes for 5, 6 or 7 anchors, so there is an important increase of the error when 5 anchors are used. Then the error slightly decreases as the ratio of recent and delayed estimated distances increases (1 recent and 4 delayed for 5 anchors, 3 recent and 4 delayed for 7 anchors). Results for multicast request (MRq SRp DA) are similar, although the error increase occurs when 6 anchors are used, as for 5 anchors the update process can be carried out within one superframe.

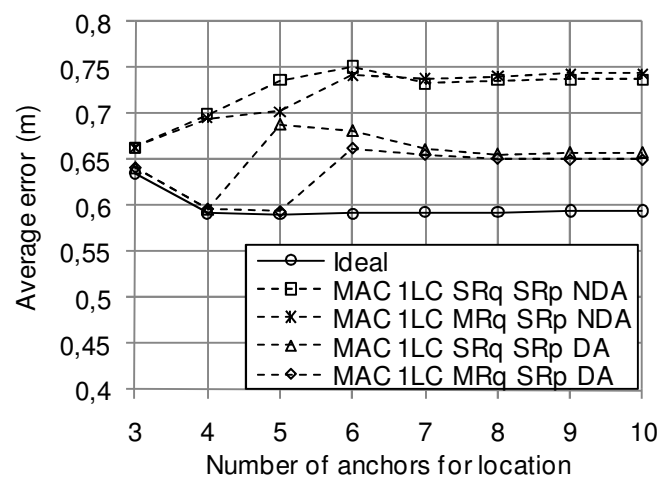


Figure 11: Average error for different acquisition & distribution modes depending on the number of anchors for location

The main conclusion is that when the update process is carried out within a single superframe, e.g. with MRq SRp DA and 3, 4 or 5 anchors, the latency is relatively small, e.g. 16 slots (59 ms), and the error increase is negligible. When the update process requires more than one superframe, latency will take values over 200 ms and the error increase is significant.

Figure 12 shows the number of slots that are needed per update for the different modes. As expected the mode with no enhancements (SRq SRp NDA) needs a higher amount of resources, and a reduction of 40% can be reached applying both multicast request and data aggregation (MRq SRp DA). The amount of slots needed is similar whether the ideal or the MAC simulator is used with one exception: when multicast request is used, the number of slots is slightly higher for the MAC simulator as in some cases multiple multicast requests will be needed depending on the availability of ranging slots for the subsequent responses.

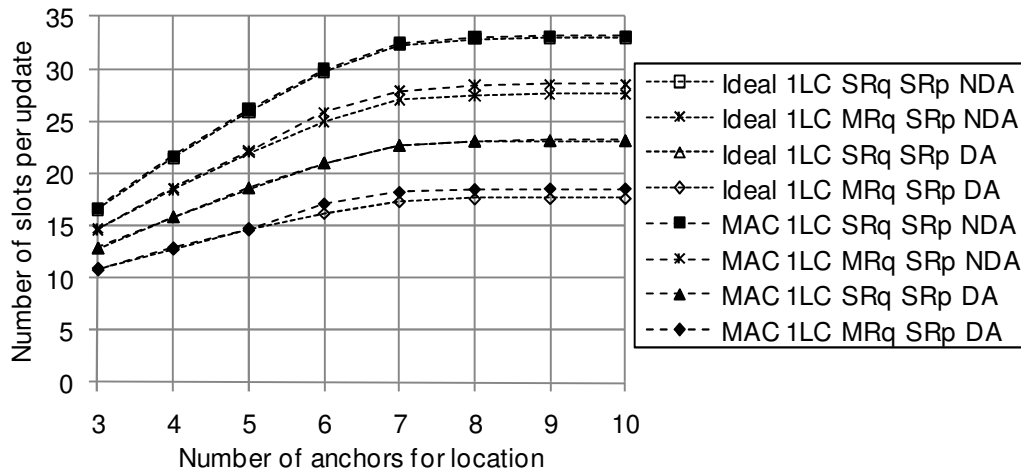


Figure 12: Number of slots per update for different acquisition & distribution modes depending on the number of anchors for location

Figure 13 shows the % of data slots that are not used for tracking and therefore are available for data transmission. This is an important measure for combined communication & tracking systems, as it measures the amount of resources that are allocated for tracking and consequently cannot be used for communication. As it can be observed, modes with data aggregation only use a 10% of data slots, so 90% are available communication, independently of the number of anchors used. Modes without data aggregation (NDA) use more data slots and only 65%-80% will be available for communication, depending on the number of anchors used for location.

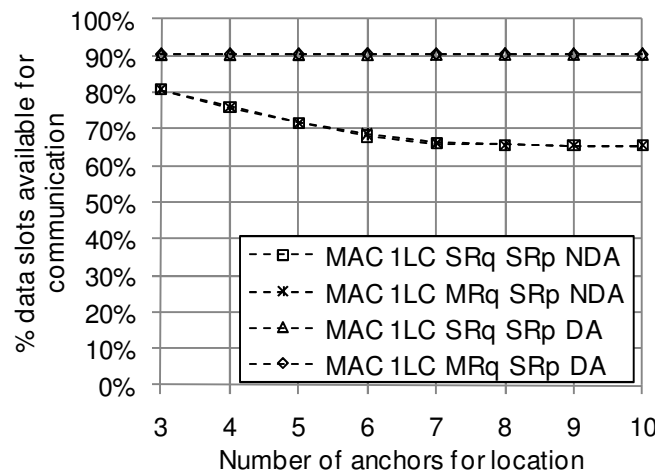


Figure 13: Data slots available for communication for different acquisition & distribution modes depending on the number of anchors for location

Now the effect of simultaneously tracking multiple targets will be analysed. With that purpose, the amount of resources needed for location have been simulated for each enhancement based on an architecture centralized in the network with one location controller (1LC), a distance between anchors of 10 meters, which results into 36 anchors, and 4 anchors used for positioning each target. The number of targets is variable. Figure 14 shows a scheme of the update process for the architecture centralized in the network with 1 LC, single request, single response and no data aggregation, depending on the number of targets. As it can be observed, the availability of data slots is the limiting factor, and the data slots will get eventually saturate when 4 or more targets are tracked.

1 target	Rq ₁₁	Rp ₁₁	Rp ₁₁	Rq ₁₂	Rp ₁₂	Rp ₁₂	Rq ₁₃	Rp ₁₃	Rp ₁₃	Rq ₁₄	Rp ₁₄	Rp ₁₄	MR ₁₁	MR ₁₁	MR ₁₂	MR ₁₂	MR ₁₃	MR ₁₃	MR ₁₄	MR ₁₄		
														PU ₁	PU ₁							
2 targets	Rq ₁₁	Rp ₁₁	Rp ₁₁	Rq ₁₂	Rp ₁₂	Rp ₁₂	Rq ₁₃	Rp ₁₃	Rp ₁₃	Rq ₁₄	Rp ₁₄	Rp ₁₄	MR ₁₁	MR ₁₁	MR ₁₂	MR ₁₂	MR ₁₃	MR ₁₃	MR ₁₄	MR ₁₄		
	Rq ₂₁	Rp ₂₁	Rp ₂₁	Rq ₂₂	Rp ₂₂	Rp ₂₂	Rq ₂₃	Rp ₂₃	Rp ₂₃	Rq ₂₄	Rp ₂₄	Rp ₂₄	PU ₁	PU ₁	MR ₂₁	MR ₂₁	MR ₂₂	MR ₂₂	MR ₂₃	MR ₂₃		
																MR ₂₄	MR ₂₄	PU ₂	PU ₂			
3 targets	Rq ₁₁	Rp ₁₁	Rp ₁₁	Rq ₁₂	Rp ₁₂	Rp ₁₂	Rq ₁₃	Rp ₁₃	Rp ₁₃	Rq ₁₄	Rp ₁₄	Rp ₁₄	MR ₁₁	MR ₁₁	MR ₁₂	MR ₁₂	MR ₁₃	MR ₁₃	MR ₁₄	MR ₁₄		
	Rq ₂₁	Rp ₂₁	Rp ₂₁	Rq ₂₂	Rp ₂₂	Rp ₂₂	Rq ₂₃	Rp ₂₃	Rp ₂₃	Rq ₂₄	Rp ₂₄	Rp ₂₄	PU ₁	PU ₁	MR ₂₁	MR ₂₁	MR ₂₂	MR ₂₂	MR ₂₃	MR ₂₃		
	Rq ₃₁	Rp ₃₁	Rp ₃₁	Rq ₃₂	Rp ₃₂	Rp ₃₂	Rq ₃₃	Rp ₃₃	Rp ₃₃	Rq ₃₄	Rp ₃₄	Rp ₃₄	MR ₂₄	MR ₂₄	PU ₂	PU ₂	MR ₃₁	MR ₃₁	MR ₃₂	MR ₃₂		
																MR ₃₃	MR ₃₃	MR ₃₄	MR ₃₄	PU ₃	PU ₃	
4 targets	Rq ₁₁	Rp ₁₁	Rp ₁₁	Rq ₁₂	Rp ₁₂	Rp ₁₂	Rq ₁₃	Rp ₁₃	Rp ₁₃	Rq ₁₄	Rp ₁₄	Rp ₁₄	MR ₁₁	MR ₁₁	MR ₁₂	MR ₁₂	MR ₁₃	MR ₁₃	MR ₁₄	MR ₁₄		
	Rq ₂₁	Rp ₂₁	Rp ₂₁	Rq ₂₂	Rp ₂₂	Rp ₂₂	Rq ₂₃	Rp ₂₃	Rp ₂₃	Rq ₂₄	Rp ₂₄	Rp ₂₄	PU ₁	PU ₁	MR ₂₁	MR ₂₁	MR ₂₂	MR ₂₂	MR ₂₃	MR ₂₃		
	Rq ₃₁	Rp ₃₁	Rp ₃₁	Rq ₃₂	Rp ₃₂	Rp ₃₂	Rq ₃₃	Rp ₃₃	Rp ₃₃	Rq ₃₄	Rp ₃₄	Rp ₃₄	MR ₂₄	MR ₂₄	PU ₂	PU ₂	MR ₃₁	MR ₃₁	MR ₃₂	MR ₃₂		
	Rq ₄₁	Rp ₄₁	Rp ₄₁	Rq ₄₂	Rp ₄₂	Rp ₄₂	Rq ₄₃	Rp ₄₃	Rp ₄₃	Rq ₄₄	Rp ₄₄	Rp ₄₄	MR ₃₃	MR ₃₃	MR ₃₄	MR ₃₄	PU ₃	PU ₃	MR ₄₁	MR ₄₁		
																MR ₄₂	MR ₄₂	MR ₄₃	MR ₄₃	MR ₄₄	MR ₄₄	PU ₄

Figure 14. Update process scheme for 1LC SRq SRp NDA depending on the number of targets

Figure 15 shows the update process scheme when data aggregation is applied (SRq SRp DA). With data aggregation the availability of data slots is not further a limitation. Every target is updated in a single superframe, and up to 5 targets could be tracked considering an update rate of 5 superframes.

1 target	Rq ₁₁	Rp ₁₁	Rp ₁₁	Rq ₁₂	Rp ₁₂	Rp ₁₂	Rq ₁₃	Rp ₁₃	Rp ₁₃	Rq ₁₄	Rp ₁₄	Rp ₁₄	MR ₁	MR ₁	PU ₁	PU ₁				
2 targets	Rq ₁₁	Rp ₁₁	Rp ₁₁	Rq ₁₂	Rp ₁₂	Rp ₁₂	Rq ₁₃	Rp ₁₃	Rp ₁₃	Rq ₁₄	Rp ₁₄	Rp ₁₄	MR ₁	MR ₁	PU ₁	PU ₁				
	Rq ₂₁	Rp ₂₁	Rp ₂₁	Rq ₂₂	Rp ₂₂	Rp ₂₂	Rq ₂₃	Rp ₂₃	Rp ₂₃	Rq ₂₄	Rp ₂₄	Rp ₂₄	MR ₂	MR ₂	PU ₂	PU ₂				
3 targets	Rq ₁₁	Rp ₁₁	Rp ₁₁	Rq ₁₂	Rp ₁₂	Rp ₁₂	Rq ₁₃	Rp ₁₃	Rp ₁₃	Rq ₁₄	Rp ₁₄	Rp ₁₄	MR ₁	MR ₁	PU ₁	PU ₁				
	Rq ₂₁	Rp ₂₁	Rp ₂₁	Rq ₂₂	Rp ₂₂	Rp ₂₂	Rq ₂₃	Rp ₂₃	Rp ₂₃	Rq ₂₄	Rp ₂₄	Rp ₂₄	MR ₂	MR ₂	PU ₂	PU ₂				
	Rq ₃₁	Rp ₃₁	Rp ₃₁	Rq ₃₂	Rp ₃₂	Rp ₃₂	Rq ₃₃	Rp ₃₃	Rp ₃₃	Rq ₃₄	Rp ₃₄	Rp ₃₄	MR ₃	MR ₃	PU ₃	PU ₃				
4 targets	Rq ₁₁	Rp ₁₁	Rp ₁₁	Rq ₁₂	Rp ₁₂	Rp ₁₂	Rq ₁₃	Rp ₁₃	Rp ₁₃	Rq ₁₄	Rp ₁₄	Rp ₁₄	MR ₁	MR ₁	PU ₁	PU ₁				
	Rq ₂₁	Rp ₂₁	Rp ₂₁	Rq ₂₂	Rp ₂₂	Rp ₂₂	Rq ₂₃	Rp ₂₃	Rp ₂₃	Rq ₂₄	Rp ₂₄	Rp ₂₄	MR ₂	MR ₂	PU ₂	PU ₂				
	Rq ₃₁	Rp ₃₁	Rp ₃₁	Rq ₃₂	Rp ₃₂	Rp ₃₂	Rq ₃₃	Rp ₃₃	Rp ₃₃	Rq ₃₄	Rp ₃₄	Rp ₃₄	MR ₃	MR ₃	PU ₃	PU ₃				
	Rq ₄₁	Rp ₄₁	Rp ₄₁	Rq ₄₂	Rp ₄₂	Rp ₄₂	Rq ₄₃	Rp ₄₃	Rp ₄₃	Rq ₄₄	Rp ₄₄	Rp ₄₄	MR ₄	MR ₄	PU ₄	PU ₄				

Figure 15. Update process scheme for 1LC SRq SRp DA depending on the number of targets

Figure 16 shows the update process scheme when both multicast request and data aggregation are applied (MRq SRp DA). Note that updates are not carried out in different superframes, but update of target #2 already starts in superframe #1 in order to make the most of the available ranging slots and increase the capacity.

1 target	Rq ₁	Rp ₁₁	Rp ₁₁	Rp ₁₂	Rp ₁₂	Rp ₁₃	Rp ₁₃	Rp ₁₄				MR ₁	MR ₁	PU ₁	PU ₁					
2 targets	Rq ₁	Rp ₁₁	Rp ₁₁	Rp ₁₂	Rp ₁₂	Rp ₁₃	Rp ₁₃	Rp ₁₄	Rp ₁₄	Rq ₂	Rp ₂₁	Rp ₂₁	MR ₁	MR ₁	PU ₁	PU ₁				
	Rq ₂	Rp ₂₂	Rp ₂₂	Rp ₂₃	Rp ₂₃	Rp ₂₄	Rp ₂₄						MR ₂	MR ₂	PU ₂	PU ₂				
3 targets	Rq ₁	Rp ₁₁	Rp ₁₁	Rp ₁₂	Rp ₁₂	Rp ₁₃	Rp ₁₃	Rp ₁₄	Rp ₁₄	Rq ₂	Rp ₂₁	Rp ₂₁	MR ₁	MR ₁	PU ₁	PU ₁				
	Rq ₂	Rp ₂₂	Rp ₂₂	Rp ₂₃	Rp ₂₃	Rp ₂₄	Rp ₂₄	Rq ₃	Rp ₃₁	Rp ₃₁	Rp ₃₂	Rp ₃₂	MR ₂	MR ₂	PU ₂	PU ₂				
	Rq ₃	Rp ₃₃	Rp ₃₃	Rp ₃₄	Rp ₃₄									MR ₃	MR ₃	PU ₃	PU ₃			
4 targets	Rq ₁	Rp ₁₁	Rp ₁₁	Rp ₁₂	Rp ₁₂	Rp ₁₃	Rp ₁₃	Rp ₁₄	Rp ₁₄	Rq ₂	Rp ₂₁	Rp ₂₁	MR ₁	MR ₁	PU ₁	PU ₁				
	Rq ₂	Rp ₂₂	Rp ₂₂	Rp ₂₃	Rp ₂₃	Rp ₂₄	Rp ₂₄	Rq ₃	Rp ₃₁	Rp ₃₁	Rp ₃₂	Rp ₃₂	MR ₂	MR ₂	PU ₂	PU ₂				
	Rq ₃	Rp ₃₃	Rp ₃₃	Rp ₃₄	Rp ₃₄	Rq ₄	Rp ₄₁	Rp ₄₁	Rp ₄₂	Rp ₄₂	Rp ₄₃	Rp ₄₃	MR ₃	MR ₃	PU ₃	PU ₃				
	Rp ₄₄	Rp ₄₄												MR ₄	MR ₄	PU ₄	PU ₄			

Figure 16. Update process scheme for 1LC MRq SRp DA depending on the number of targets

Finally, Figure 17 shows the update process scheme when all the enhancements are applied (MRq MRp DA). Note that now ranging responses are not sent per each target-anchor pair, but per each anchor. Some anchors may be used by multiple targets, so in general the amount of responses and consequently the number of ranging slots will decrease, thus increasing the capacity.

1 target	Rq ₁	Rp ₁	Rp ₁	Rp ₂	Rp ₂	Rp ₃	Rp ₃	Rp ₄	Rp ₄				MR ₁	MR ₁	PU ₁	PU ₁				
2 targets	Rq ₁	Rq ₂	Rp ₁	Rp ₁	Rp ₂	Rp ₂	Rp ₃	Rp ₃	Rp ₄	Rp ₄	Rp ₅	Rp ₅	MR ₁	MR ₁	PU ₁	PU ₁				
	Rp ₆	Rp ₆	Rp ₇	Rp ₇									MR ₂	MR ₂	PU ₂	PU ₂				
3 targets	Rq ₁	Rq ₂	Rq ₃	Rp ₁	Rp ₁	Rp ₂	Rp ₂	Rp ₃	Rp ₃	Rp ₄	Rp ₄		MR ₁	MR ₁	PU ₁	PU ₁				
	Rp ₅	Rp ₅	Rp ₆	Rp ₆	Rp ₇	Rp ₇	Rp ₈	Rp ₈	Rp ₉	Rp ₉	Rp ₁₀	Rp ₁₀	MR ₂	MR ₂	PU ₂	PU ₂	MR ₃	MR ₃	PU ₃	PU ₃
	Rp ₁₁	Rp ₁₁											MR ₃	MR ₃	PU ₃	PU ₃				
4 targets	Rq ₁	Rq ₂	Rq ₃	Rq ₄	Rp ₁	Rp ₁	Rp ₂	Rp ₂	Rp ₃	Rp ₃	Rp ₄	Rp ₄	MR ₁	MR ₁	PU ₁	PU ₁				
	Rp ₅	Rp ₅	Rp ₆	Rp ₆	Rp ₇	Rp ₇	Rp ₈	Rp ₈	Rp ₉	Rp ₉	Rp ₁₀	Rp ₁₀	MR ₂	MR ₂	PU ₂	PU ₂				
	Rp ₁₁	Rp ₁₁	Rp ₁₂	Rp ₁₂	Rp ₁₃	Rp ₁₃	Rp ₁₄	Rp ₁₄					MR ₃	MR ₃	PU ₃	PU ₃	MR ₄	MR ₄	PU ₄	PU ₄

Figure 17. Update process scheme for 1LC MRq MRp DA depending on the number of targets

The average error for the different modes depending on the number of targets is shown in Figure 18. For the mode with no enhancements (SRq SRp NDA) the error grows exponentially, as there are not enough data slots and latency increases as the number of targets grows. For more than 4 targets, the data slots are completely saturated, which entails that the latency increases on every update until it stabilizes between 800-1000 ms (4-5 superframes) and the error can be as high as 2 m. When data aggregation is used (SRq SRp DA) every update is carried out in a single superframe, so the error is just slightly higher than the ideal simulator. For 6 or more targets, there will be not enough superframes and the actual time between updates will increase. This entails a delay between the selection of the anchors and the update process, and consequently a slight increase of the error.

When both multicast request and data aggregation are applied (MRq SRp DA), the error increases as the number of targets grow, as the update of target #2 starts in superframe #1 and finishes in superframe #2, update of target #3 starts in superframe #2 and finishes in superframe #3, and update of

target #4 starts in superframe #3 and finishes in superframe #4, as it can be observed in Figure 16. For 5 and 6 anchors there is no increase, as update of target #5 would take place in superframe #4 and update of target #6 would take place in superframe #5. For 7 and more targets we would have a further increase.

Finally, when all the enhancements are applied (MRq MRp DA), the behaviour is difficult to predict, as it depends on how many anchors are shared between the targets and how the ranging exchanges are coordinated, but in general the average latency of the updates will be a little bit higher and so will be the average error. For more than 6 targets there is an important increase of the error, and ranging exchanges may typically finish in the fifth superframe and there may be not enough data slots to transmit the location information for the remaining targets, which may be delayed one or more superframes.

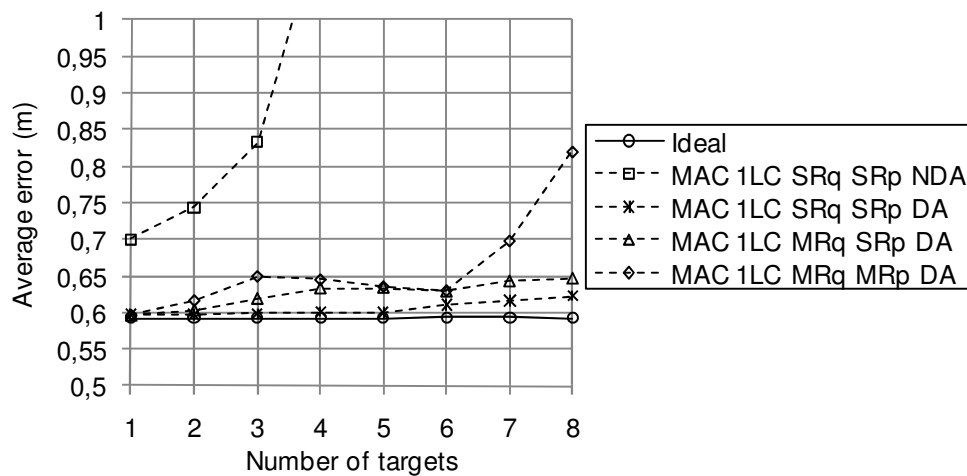


Figure 18: Average error for different acquisition & distribution modes depending on the number of targets

Figure 19 shows the actual time between updates in order to identify when each mode is saturated. The mode without enhancements (SRq SRp NDA) can track up to 3 targets and data slots get saturated for 4 targets. With data aggregation (SRq SRp DA), up to 5 targets can be tracked before ranging slots are saturated. With multicast ranging and data aggregation (MRq SRp DA), up to 6 targets can be tracked, and when all the enhancements are applied up to 8 targets can be simultaneously tracked (MRq MRp DA).

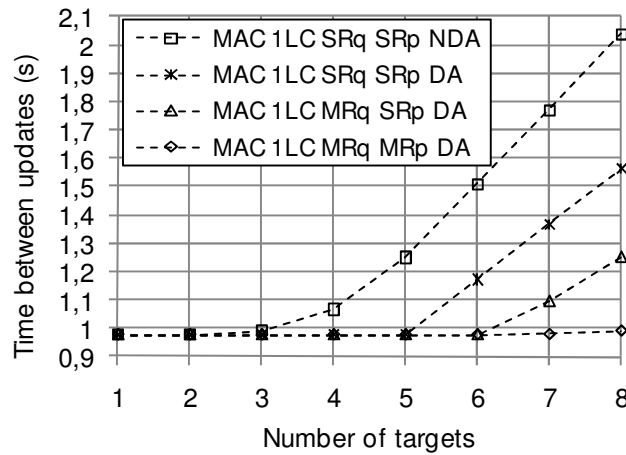


Figure 19: Time between updates for different acquisition & distribution modes depending on the number of targets

Figure 20 shows the % of slots available for communication. As it was previously commented, when no enhancements are applied, data slots are saturated for more than 4 anchors, with a residual 10% left for data communication. For the enhanced modes, the % of slots available decreases linearly as the number of targets increases, until they get saturated due to the limitation of ranging slots.

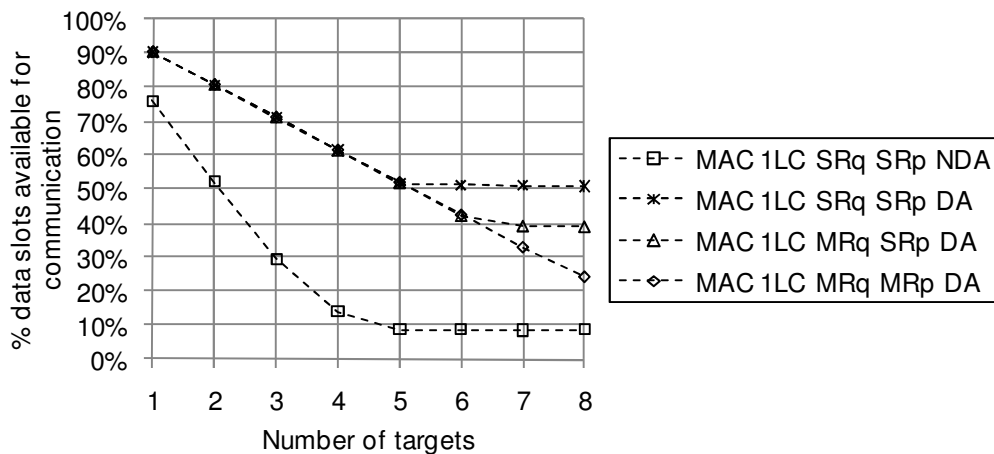


Figure 20: Data slots available for communication for different acquisition & distribution modes depending on the number of targets

In order to show the limitation due to the availability of ranging slots, Figure 21 shows the % of ranging slots used for each mode depending on the number of targets. As it can be observed, with no enhancements a full use of the ranging slots is not reached as it is limited by the unavailability of data slots. For the SRq SRp DA mode the % of ranging slots used increases linearly until 5 targets, when ranging slots gets saturated. It reaches a full usage of ranging slots, as each update uses exactly the 12 ranging slots available on each superframe, as it can be observed in Figure 15. The modes with multicast request and multicast response use less ranging slots so they can track a higher number of targets. These modes do not reach a full usage, as there may be residual slots on some superframes.

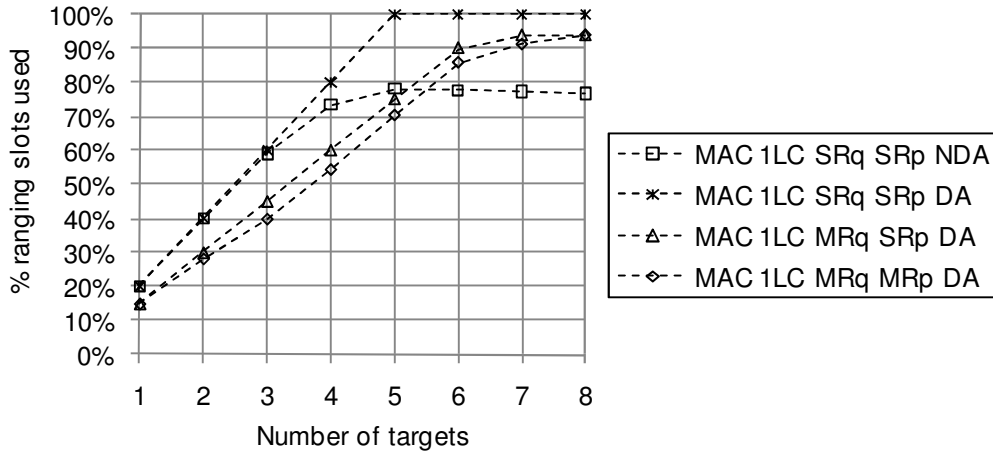


Figure 21: Ranging slots used for different acquisition & distribution modes depending on the number of targets

2.2.3.2 Impact of the tracking system architecture

As it was previously explained, the tracking functionality is executed by the location controllers, which can be physically implemented in one or more anchor nodes or in the mobile nodes, depending on the architecture that is defined.

As in the previous section, first we are presenting the update process schemes for the different architectures depending on the number of anchors used for location. A SRq SRp NDA mode has been considered. The scheme for the architecture centralized in the network was already presented in Figure 7. Figure 22 shows the scheme for a distributed architecture. Note that now only one slot is allocated to each data frame (MR and PU), as the LC functionality will be always executed by an anchor neighbour to the target. Figure 23 shows the scheme for an architecture centralized in the mobile nodes. In this case, the target computes its own position, so there is no need of using data frames for transmitting the distances and the position, and position can be computed right after the last distance is estimated.

3 anchors	Rq ₁₁	Rp ₁₁	Rp ₁₁	Rq ₁₂	Rp ₁₂	Rp ₁₂	Rq ₁₃	Rp ₁₃	Rp ₁₃				MR ₁₁	MR ₁₂	MR ₁₃	PU ₁					
4 anchors	Rq ₁₁	Rp ₁₁	Rp ₁₁	Rq ₁₂	Rp ₁₂	Rp ₁₂	Rq ₁₃	Rp ₁₃	Rp ₁₃	Rq ₁₄	Rp ₁₄	Rp ₁₄	MR ₁₁	MR ₁₂	MR ₁₃	MR ₁₄	PU ₁				
5 anchors	Rq ₁₁	Rp ₁₁	Rp ₁₁	Rq ₁₂	Rp ₁₂	Rp ₁₂	Rq ₁₃	Rp ₁₃	Rp ₁₃	Rq ₁₄	Rp ₁₄	Rp ₁₄	MR ₁₁	MR ₁₂	MR ₁₃	MR ₁₄					
	Rq ₁₅	Rp ₁₅	Rp ₁₅										MR ₁₅	PU ₁							
6 anchors	Rq ₁₁	Rp ₁₁	Rp ₁₁	Rq ₁₂	Rp ₁₂	Rp ₁₂	Rq ₁₃	Rp ₁₃	Rp ₁₃	Rq ₁₄	Rp ₁₄	Rp ₁₄	MR ₁₁	MR ₁₂	MR ₁₃	MR ₁₄					
	Rq ₁₅	Rp ₁₅	Rp ₁₅	Rq ₁₆	Rp ₁₆	Rp ₁₆							MR ₁₅	MR ₁₆	PU ₁						
7 anchors	Rq ₁₁	Rp ₁₁	Rp ₁₁	Rq ₁₂	Rp ₁₂	Rp ₁₂	Rq ₁₃	Rp ₁₃	Rp ₁₃	Rq ₁₄	Rp ₁₄	Rp ₁₄	MR ₁₁	MR ₁₂	MR ₁₃	MR ₁₄					
	Rq ₁₅	Rp ₁₅	Rp ₁₅	Rq ₁₆	Rp ₁₆	Rp ₁₆	Rq ₁₇	Rp ₁₇	Rp ₁₇				MR ₁₅	MR ₁₆	MR ₁₇	PU ₁					

Figure 22. Update process scheme for Distributed SRq SRp NDA depending on the number of anchors

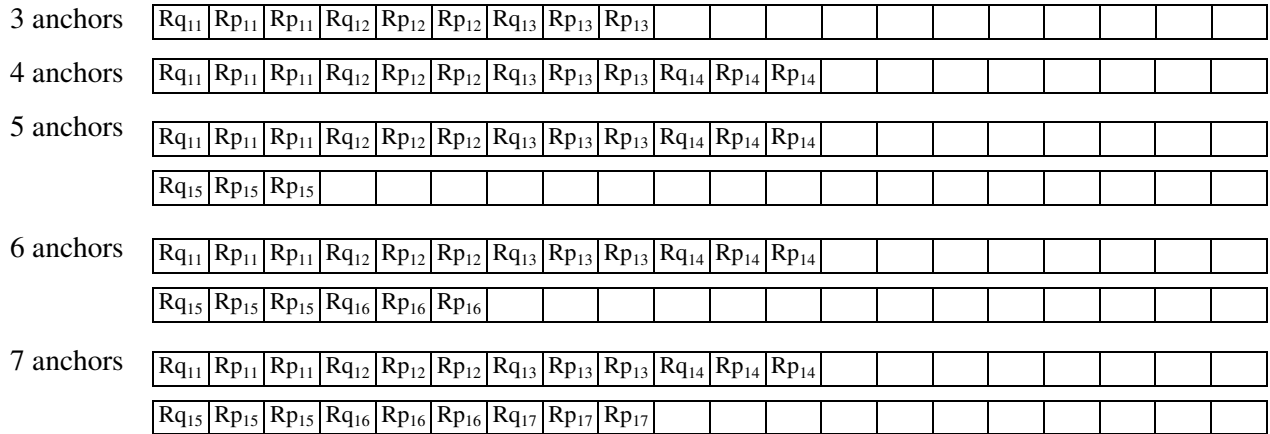


Figure 23. Update process scheme for Mobile SRq SRp NDA depending on the number of anchors

Figure 24 shows the average error obtained for the different architectures depending on the number of anchors used for location. Results for the architecture centralized in the network with 1 location controller (1LC) where already discussed in previous section. For the distributed architecture, the limitation is due to the ranging exchanges, as data frames transmission can always be done within a superframe. Consequently there is an important increase of the error when 5 anchors are used, as a second superframe will be needed, and a slight decrease for more anchors. A slightly higher error level is obtained for an architecture centralized in the network with 4 LC, as most of time the target will be neighbour to one of the location controllers. Finally, the architecture centralized in the mobile nodes shows a similar evolution but with a slightly lower error, as the position can be computed as the last distance is estimated, so the latency of the update process will always be a little bit shorter.

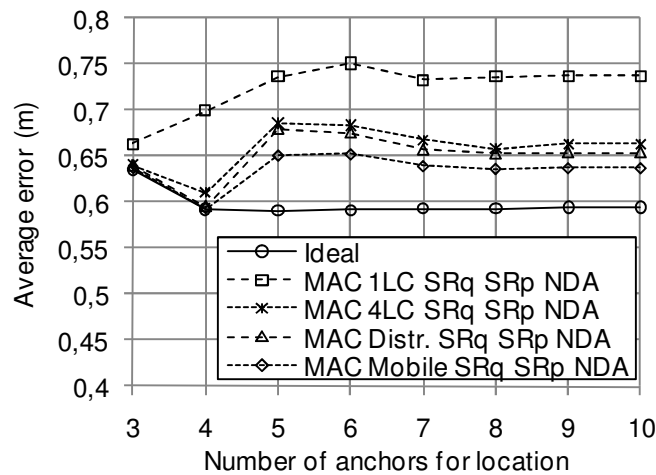


Figure 24: Average error for different tracking architectures depending on the number of anchors for location (mode SRq SRp NDA)

Figure 25 shows the number of slots per update for the different architectures and a SRq SRp NDA mode. As expected, the architecture centralized in the network with 1 location controller has the highest need of resources. With the distributed architecture, the amount of resources needed is reduced in approximately a 20%, and similar results can be obtained using an architecture centralized in the network with 4 location controllers. Finally, the architecture centralized in the mobile nodes is optimum in terms of resources as a reduction of approximately 40% in the amount of slots is obtained.

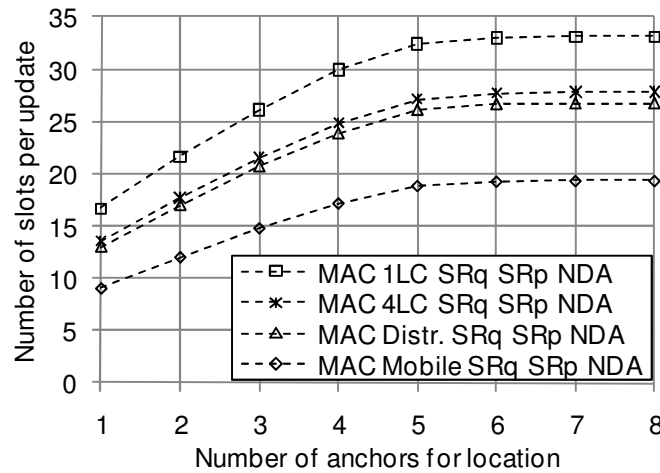


Figure 25: Number of slots per update for different tracking architectures depending on the number of anchors for location (mode SRq SRp NDA)

Concerning the % of data slots available for data communication, results are shown in Figure 26. As the architecture centralized in the mobile nodes does not need the transmission of location information, 100% of the data slots are available for communication. With the architecture centralized in the network with 1 location controller, only 65%-80% of the data slots would be available for data transmission, whereas using 4 location controllers or a distributed architecture 80%-90% of the data slots are available for communication, depending on the number of anchors used for location.

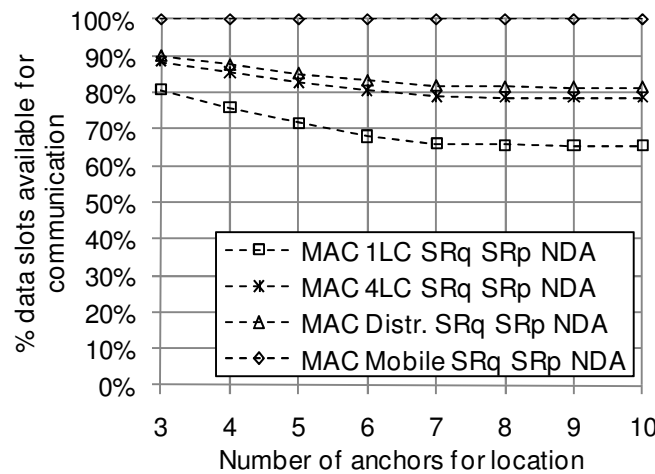


Figure 26: Data slots available for communication for different tracking architectures depending on the number of anchors for location (mode SRq SRp NDA)

Following, the impact of the tracking architecture is analysed depending on the number of targets that are simultaneously tracked. A SRq SRp NDA mode was considered. The update process scheme for the architecture centralized in the network was already presented in Figure 14. Figure 27 shows the update process scheme for the distributed architecture. Note that only 1 slot is needed to transmit the location data frames (MR and PU), as the LC functionality is always executed by an anchor neighbour to the target. Figure 28 shows the update process scheme for the architecture centralized in the mobile. Note that no location data transmission is needed, as the mobile computes its own position.

1 target	Rq ₁₁	Rp ₁₁	Rp ₁₁	Rq ₁₂	Rp ₁₂	Rp ₁₂	Rq ₁₃	Rp ₁₃	Rp ₁₃	Rq ₁₄	Rp ₁₄	Rp ₁₄	MR ₁₁	MR ₁₂	MR ₁₃	MR ₁₄	PU ₁			
2 targets	Rq ₁₁	Rp ₁₁	Rp ₁₁	Rq ₁₂	Rp ₁₂	Rp ₁₂	Rq ₁₃	Rp ₁₃	Rp ₁₃	Rq ₁₄	Rp ₁₄	Rp ₁₄	MR ₁₁	MR ₁₂	MR ₁₃	MR ₁₄	PU ₁			
	Rq ₂₁	Rp ₂₁	Rp ₂₁	Rq ₂₂	Rp ₂₂	Rp ₂₂	Rq ₂₃	Rp ₂₃	Rp ₂₃	Rq ₂₄	Rp ₂₄	Rp ₂₄	MR ₂₁	MR ₂₂	MR ₂₃	MR ₂₄	PU ₂			
3 targets	Rq ₁₁	Rp ₁₁	Rp ₁₁	Rq ₁₂	Rp ₁₂	Rp ₁₂	Rq ₁₃	Rp ₁₃	Rp ₁₃	Rq ₁₄	Rp ₁₄	Rp ₁₄	MR ₁₁	MR ₁₂	MR ₁₃	MR ₁₄	PU ₁			
	Rq ₂₁	Rp ₂₁	Rp ₂₁	Rq ₂₂	Rp ₂₂	Rp ₂₂	Rq ₂₃	Rp ₂₃	Rp ₂₃	Rq ₂₄	Rp ₂₄	Rp ₂₄	MR ₂₁	MR ₂₂	MR ₂₃	MR ₂₄	PU ₂			
	Rq ₃₁	Rp ₃₁	Rp ₃₁	Rq ₃₂	Rp ₃₂	Rp ₃₂	Rq ₃₃	Rp ₃₃	Rp ₃₃	Rq ₃₄	Rp ₃₄	Rp ₃₄	MR ₃₁	MR ₃₂	MR ₃₃	MR ₃₄	PU ₃			
4 targets	Rq ₁₁	Rp ₁₁	Rp ₁₁	Rq ₁₂	Rp ₁₂	Rp ₁₂	Rq ₁₃	Rp ₁₃	Rp ₁₃	Rq ₁₄	Rp ₁₄	Rp ₁₄	MR ₁₁	MR ₁₂	MR ₁₃	MR ₁₄	PU ₁			
	Rq ₂₁	Rp ₂₁	Rp ₂₁	Rq ₂₂	Rp ₂₂	Rp ₂₂	Rq ₂₃	Rp ₂₃	Rp ₂₃	Rq ₂₄	Rp ₂₄	Rp ₂₄	MR ₂₁	MR ₂₂	MR ₂₃	MR ₂₄	PU ₂			
	Rq ₃₁	Rp ₃₁	Rp ₃₁	Rq ₃₂	Rp ₃₂	Rp ₃₂	Rq ₃₃	Rp ₃₃	Rp ₃₃	Rq ₃₄	Rp ₃₄	Rp ₃₄	MR ₃₁	MR ₃₂	MR ₃₃	MR ₃₄	PU ₃			
	Rq ₄₁	Rp ₄₁	Rp ₄₁	Rq ₄₂	Rp ₄₂	Rp ₄₂	Rq ₄₃	Rp ₄₃	Rp ₄₃	Rq ₄₄	Rp ₄₄	Rp ₄₄	MR ₄₁	MR ₄₂	MR ₄₃	MR ₄₄	PU ₄			

Figure 27. Update process scheme for Distributed SRq SRp NDA depending on the number of targets

1 target	Rq ₁₁	Rp ₁₁	Rp ₁₁	Rq ₁₂	Rp ₁₂	Rp ₁₂	Rq ₁₃	Rp ₁₃	Rp ₁₃	Rq ₁₄	Rp ₁₄	Rp ₁₄								
2 targets	Rq ₁₁	Rp ₁₁	Rp ₁₁	Rq ₁₂	Rp ₁₂	Rp ₁₂	Rq ₁₃	Rp ₁₃	Rp ₁₃	Rq ₁₄	Rp ₁₄	Rp ₁₄								
	Rq ₂₁	Rp ₂₁	Rp ₂₁	Rq ₂₂	Rp ₂₂	Rp ₂₂	Rq ₂₃	Rp ₂₃	Rp ₂₃	Rq ₂₄	Rp ₂₄	Rp ₂₄								
3 targets	Rq ₁₁	Rp ₁₁	Rp ₁₁	Rq ₁₂	Rp ₁₂	Rp ₁₂	Rq ₁₃	Rp ₁₃	Rp ₁₃	Rq ₁₄	Rp ₁₄	Rp ₁₄								
	Rq ₂₁	Rp ₂₁	Rp ₂₁	Rq ₂₂	Rp ₂₂	Rp ₂₂	Rq ₂₃	Rp ₂₃	Rp ₂₃	Rq ₂₄	Rp ₂₄	Rp ₂₄								
	Rq ₃₁	Rp ₃₁	Rp ₃₁	Rq ₃₂	Rp ₃₂	Rp ₃₂	Rq ₃₃	Rp ₃₃	Rp ₃₃	Rq ₃₄	Rp ₃₄	Rp ₃₄								
4 targets	Rq ₁₁	Rp ₁₁	Rp ₁₁	Rq ₁₂	Rp ₁₂	Rp ₁₂	Rq ₁₃	Rp ₁₃	Rp ₁₃	Rq ₁₄	Rp ₁₄	Rp ₁₄								
	Rq ₂₁	Rp ₂₁	Rp ₂₁	Rq ₂₂	Rp ₂₂	Rp ₂₂	Rq ₂₃	Rp ₂₃	Rp ₂₃	Rq ₂₄	Rp ₂₄	Rp ₂₄								
	Rq ₃₁	Rp ₃₁	Rp ₃₁	Rq ₃₂	Rp ₃₂	Rp ₃₂	Rq ₃₃	Rp ₃₃	Rp ₃₃	Rq ₃₄	Rp ₃₄	Rp ₃₄								
	Rq ₄₁	Rp ₄₁	Rp ₄₁	Rq ₄₂	Rp ₄₂	Rp ₄₂	Rq ₄₃	Rp ₄₃	Rp ₄₃	Rq ₄₄	Rp ₄₄	Rp ₄₄								

Figure 28. Update process scheme for Mobile SRq SRp NDA depending on the number of targets

The average error for the different tracking architectures depending on the number of targets is shown in Figure 29. As it was already explained in the previous section, the error for the architecture centralized in the network with 1 LC grows exponentially as the number of targets increases, as there are not enough data slots available. Concerning the architectures distributed and centralized in the mobile, every update process is carried out within a single superframe, so the error is very similar to the ideal. Only for 6 or more targets the error increases, as the ranging slots get saturated, thus increasing the actual time between updates and causing a delay between the anchor selection and the actual start of the ranging exchanges. A similar evolution is shown with an architecture centralized in the network with 4 location controllers but with a slightly higher error level, as most of the time the target will be neighbour to a LC, but sometimes it will need 2 hops to reach the LC and the update process will then need 2 superframes, thus increasing the latency and the average error.

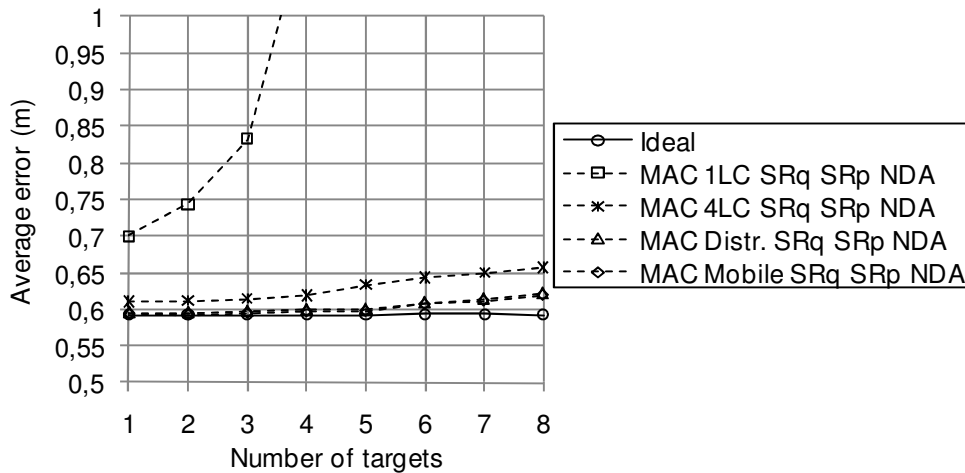


Figure 29: Average error for different tracking architectures depending on the number of targets (mode SRq SRp NDA)

The actual time between updates can be observed in Figure 30. As it was commented in the previous section, with the architecture centralized in the network with 1 LC and SRq SRp NDA mode the data slots are saturated for 4 or more targets, so the actual time between updates increases. For the other modes, the limiting factor is the availability of ranging slots, so for an update rate of 1 update every 5 superframes up to 5 targets can be simultaneously tracked.

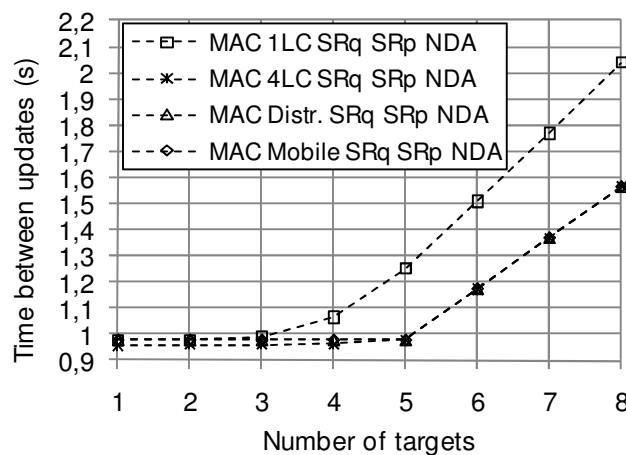


Figure 30: Time between updates for different tracking architectures depending on the number of targets (mode SRq SRp NDA)

Figure 31 shows the amount of data slots available for communication. As the architecture centralized in the mobiles does not need location data transmission, 100% of data slots are always available for communication. On the other hand data slots for the architecture centralized in the network with 1 location controller gets saturated for more than 4 targets, leaving only a residual 10% of data slots available. Finally, for the architectures distributed and centralized in the network with 4 location controllers the % of data slots available for communication decreases linearly as the number of targets increases until 5 targets, when ranging slots get saturated.

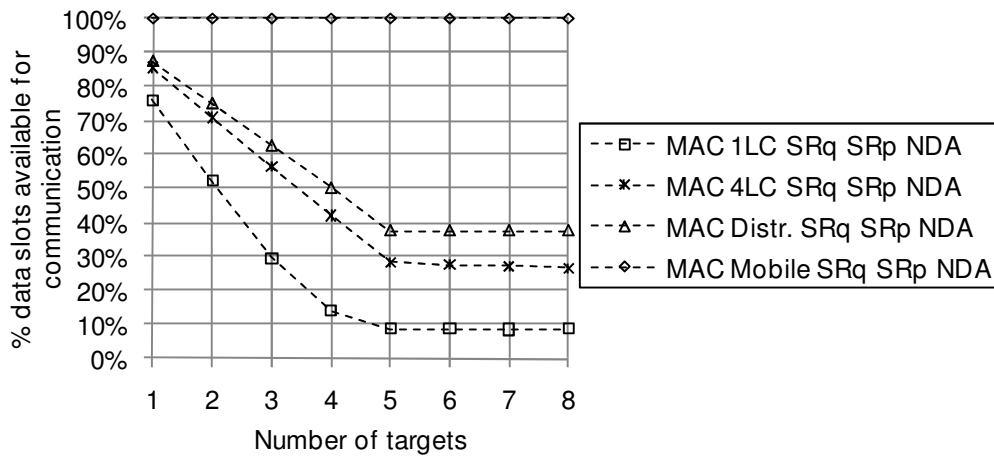


Figure 31: Data slots available for communication for different tracking architectures depending on the number of targets (mode SRq SRp NDA)

Concerning the ranging slots, Figure 32 shows the % of ranging slots used. It can be observed that the architecture centralized in the network with 1 LC controller does not reach a full use of ranging slots as it gets saturated for more than 4 targets due to the unavailability of data slots. For the rest of architectures considered, ranging slots get saturated for 5 or more targets with a full use of ranging slots.

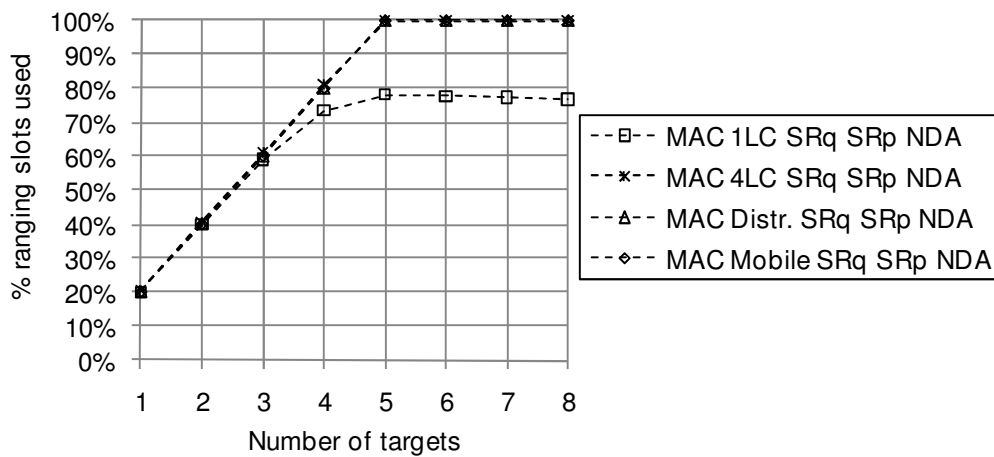


Figure 32: Ranging slots used for different tracking architectures depending on the number of targets (mode SRq SRp NDA)

Following, a similar comparison between the architectures is done but considering an enhanced mode featuring multicast request and data aggregation (MRq SRp DA). Multicast response has not been considered as it requires some coordination that is only feasible with the architecture centralized in the network. The update process scheme for the architecture centralized in the network with one LC was already shown in Figure 10. Figure 33 and Figure 34 show the schemes for the distributed architecture and the architecture centralized in the mobile nodes respectively.

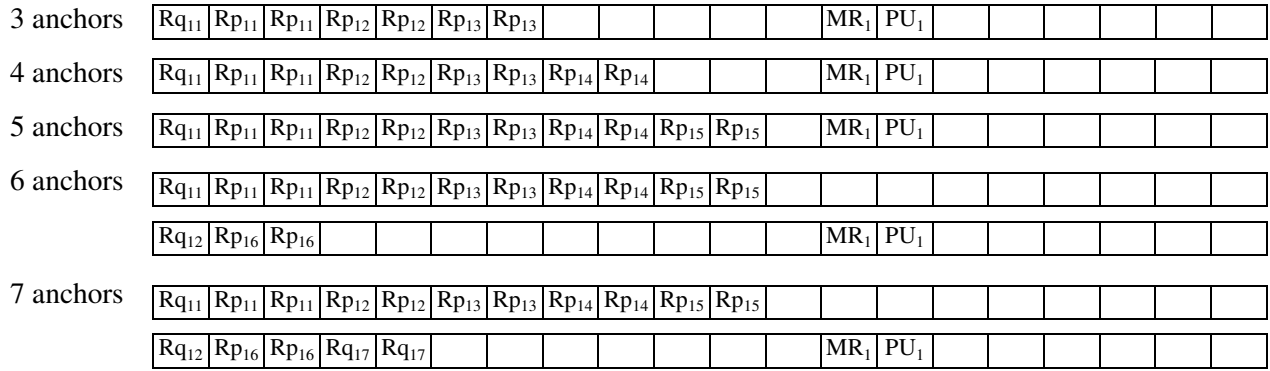


Figure 33. Update process scheme for Distributed MRq SRp DA depending on the number of anchors

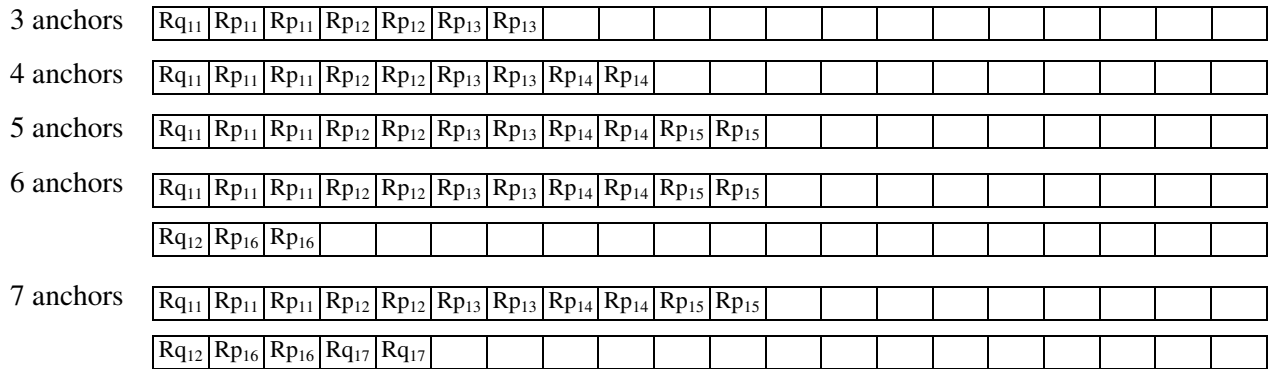


Figure 34. Update process scheme for Mobile MRq SRp DA depending on the number of anchors

Figure 35 shows the average error obtained for the different architectures with a MRq SRp DA mode. With this mode, all the architectures are limited by the ranging exchanges, so they all show a similar evolution with an error increase when 6 anchors are used as a second superframe will be needed. On the other hand, the architecture centralized in the mobile nodes shows a slightly lower average error as the position is computed right after the last distance is estimated and consequently latency is always a little shorter.

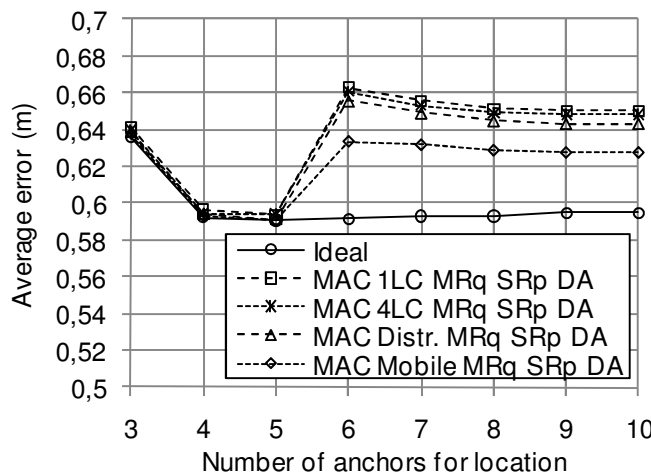


Figure 35: Average error for different tracking architectures depending on the number of anchors for location (mode MRq SRp DA)

Figure 36 shows the number of slots per update for the different architectures. The architecture centralized in the mobile nodes shows again the best results, although now the differences between the

different architectures is smaller as data aggregation reduces the amount of data frames needed for the transmission of the estimated distances.

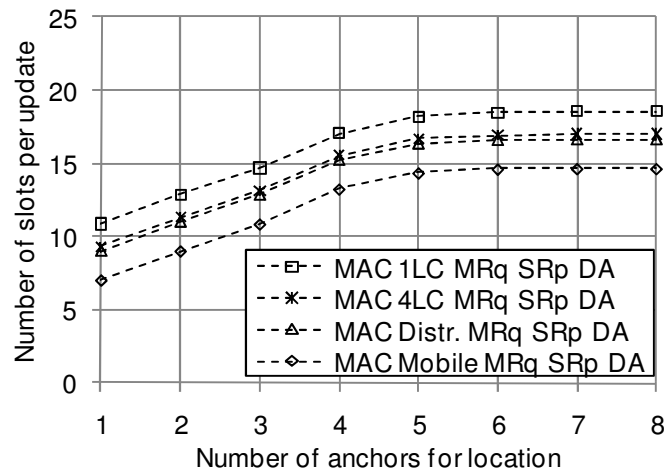


Figure 36: Number of slots per update for different tracking architectures depending on the number of anchors for location (mode MRq SRp DA)

The % of data slots available for communication is shown in Figure 37. As the architecture centralized in the mobile nodes does not need the transmission of location information, 100% of the data slots are available for communication. Nevertheless, thanks to the use of data aggregation, the amount of data slots used for location is reduced for the rest of the architectures and always more than 90% of the data slots are available for data communication independently of the number of anchors used for location.

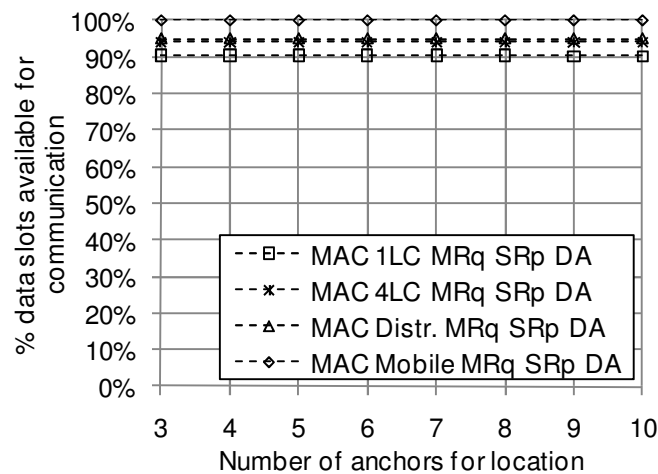


Figure 37: Data slots available for communication for different tracking architectures depending on the number of anchors for location (mode MRq SRp DA)

Finally, the performance of the different architectures with an enhanced MRq SRp DA mode is going to be analysed depending on the number targets to be tracked. The update process scheme for the architecture centralized in the network was already presented in Figure 17. Figure 38 and Figure 39 show the update process scheme for the architectures distributed and centralized in the mobiles respectively.

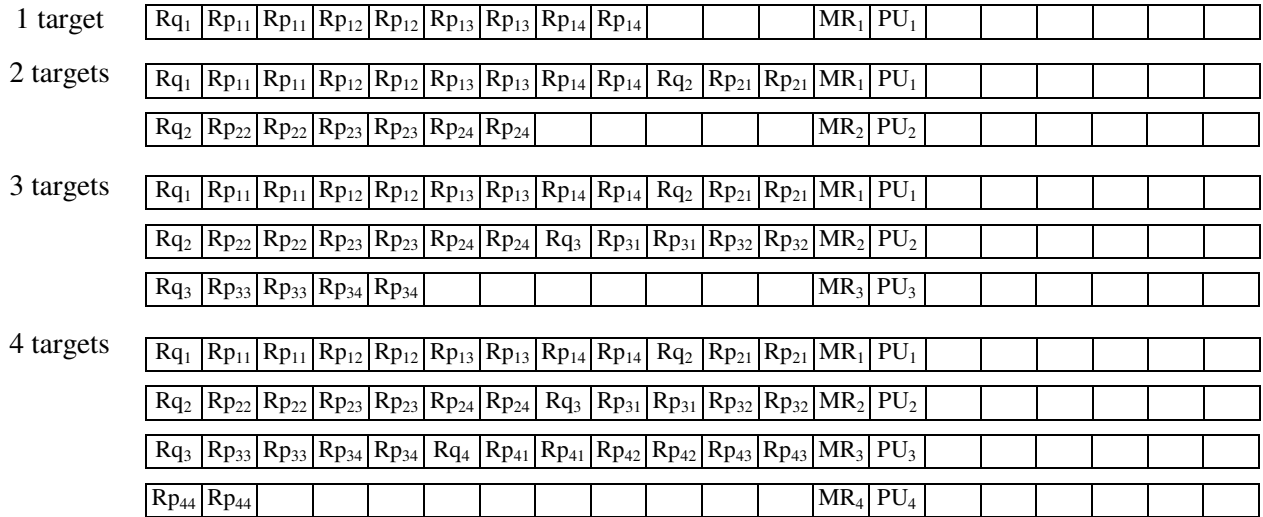


Figure 38. Update process scheme for Distributed MRq SRp DA depending on the number of targets

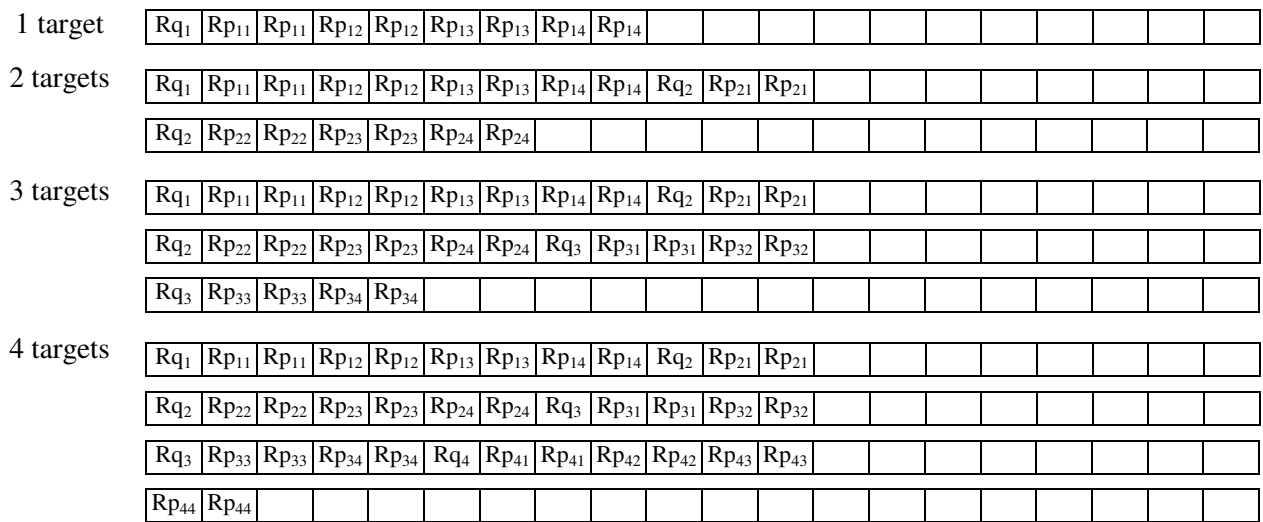


Figure 39. Update process scheme for Mobile MRq SRp DA depending on the number of targets

Figure 40 shows the average error for the different architectures considered for a MRq SRp NDA mode depending on the number of targets. As it can be observed, the architectures centralized in the network with 1 LC, distributed and centralized in the mobile nodes all have a similar evolution. As it can be observed in Figure 17, Figure 38 and Figure 39, the update of target #1 takes place in superframe #1 so the error for 1 target will be just slightly higher than the ideal. The update of target #2 starts in superframe #1 and finishes in superframe #2, update of target #3 starts in superframe #2 and finishes in superframe #3, and update of target #4 starts in superframe #3 and finishes in superframe #4, so updates of targets #2, #3 and #4 have a higher latency and the error increases as 2, 3 and 4 targets are tracked. For 5 and 6 anchors there is no increase, as update of target #5 would take place in superframe #4 and update of target #6 would take place in superframe #5. For 7 and more targets there would be a further increase. The architecture centralized in mobile nodes presents a smaller error as position can be computed as soon as the last distance is estimated, so its latency is the smallest, whereas the architecture centralized in the network with 1 LC shows a higher error as multiple slots may be needed to relay the location data frames, so its latency is the highest. On the other hand, the architecture centralized in the network with 4 location controllers does not show that behaviour but a more regular increase. This is due to the fact that when multiple location controllers

are used position updates are not completely periodic, as there are also asynchronous updates when a target changes from one LC to another, thus randomizing the timing of the updates.

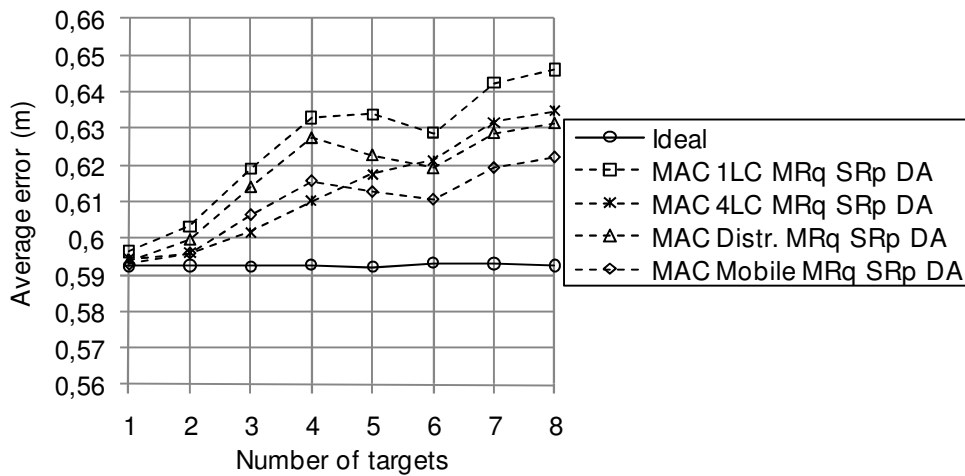


Figure 40: Average error for different tracking architectures depending on the number of targets (mode MRq SRp DA)

Concerning the actual time between updates, with all the architectures up to 6 targets can be tracked, as it can be observed in Figure 41. Note that actual time between updates for the architecture centralized in the network with 4 location controllers is slightly smaller due to the asynchronous updates happening when a target moves from one LC to another.

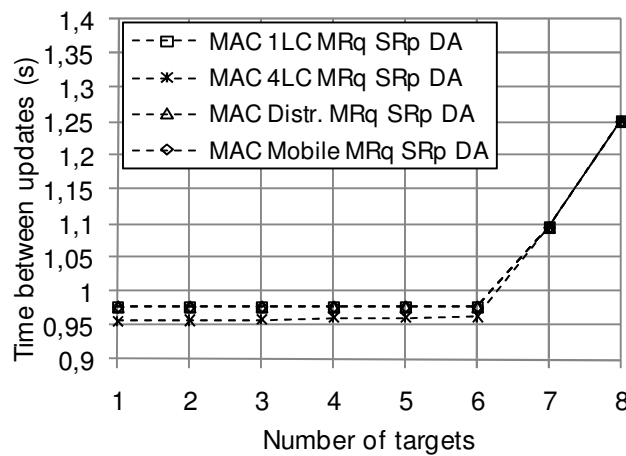


Figure 41: Time between updates for different tracking architectures depending on the number of targets (mode MRq SRp DA)

Figure 42 shows the % of data slots available for data communication. As the architecture centralized in the mobile nodes does not need location data transmission, 100% of data slots are always available for communication. For the other architectures, the % of data slots available for communication decreases linearly as the number of targets increases until 6 targets, when ranging slots get saturated. Then only 40% of data slots are available for communication with the architecture centralized in the network with 1 LC, compared to the 60%-70% available with the architectures centralized in the network with 4 LC and distributed and the full availability with the architecture centralized in the mobile nodes.

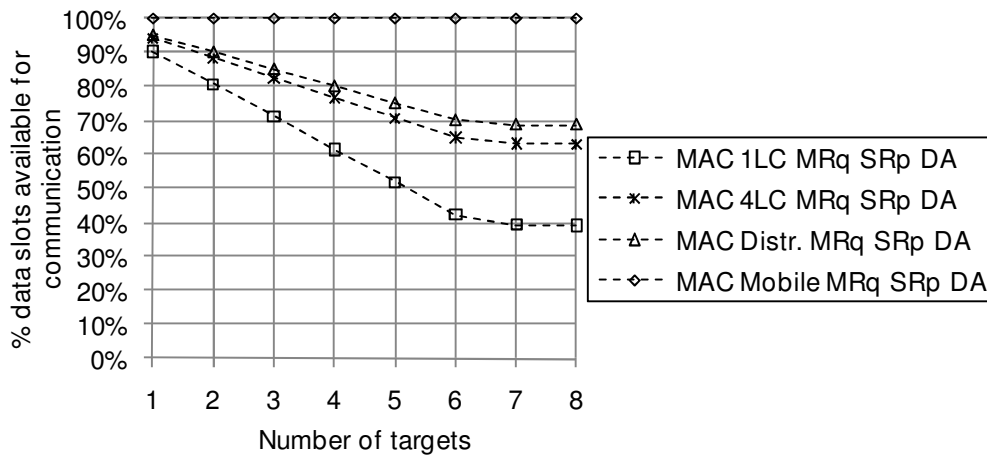


Figure 42: Data slots available for communication for different tracking architectures depending on the number of targets (mode MRq SRp DA)

Finally, Figure 43 shows the % of ranging slots used. As it can be observed, for all the architectures ranging slots get saturated for 6 or more targets, although a full usage is not reached and there is a residual 5% of slots that are not used.

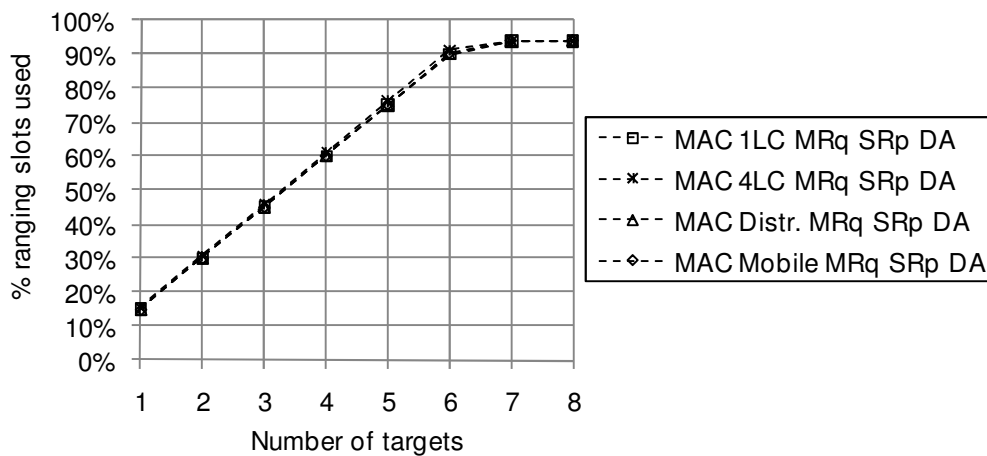


Figure 43: Ranging slots used for different tracking architectures depending on the number of targets (mode MRq SRp DA)

2.2.3.3 Conclusions

In the design of a UWB combined communication and tracking system in the framework of IEEE 802.15.4a, as the LDR-LT platform developed within EUWB WP7, the timing and structure of the MAC layer must be taken into account, as the delay and the limitation of resources impact not only on the capacity of the communication systems, but also on the accuracy and the capacity of the tracking system.

As it was demonstrated through several simulations, the positioning error is sensitive to the latency of the position update process, and specifically the delay between the distance estimation and the position computation. If the position update process is carried out within a single superframe, this latency is relatively small and the error increase is negligible. But if the position update process covers multiple superframes, the latency will be over 200 ms and the error increase is significant.

Also the limitation in resources, specifically the number of slots allocated for ranging and data transmission on each superframe, entails a limitation of the number of targets that can be tracked simultaneously. Furthermore, the allocation of resources to the tracking functionality results in a reduction of the resources available for communications.

Consequently, the design of the tracking functionality must take into account these effects and implement suitable architectures and location information acquisition and distribution strategies that reduce the position update latency and the amount of resources used. The architecture centralized in the mobile nodes is optimal in terms of latency and resources needed, as there is no need of transmitting the estimated distances to the network. Nevertheless it requires some computational capacity on the mobile targets in order to calculate their own position. If an architecture centralized in the network is used, the use of data aggregation for the transmission of the distances to the location controller is mandatory in order to reduce the amount of data slots needed. Finally, a flexible allocation of ranging slots within the GTS period is preferred over a fixed one, in order to assure that there are enough slots to complete the update on a single superframe and, on the other hand, guarantee that there are not idle ranging slots, thus optimizing the amount of resources available for data communication.

2.2.4 Impact on Radio Resource Management

Radio Resource Management (RRM) comprises different system-level strategies and algorithms aiming to use the limited radio spectrum resources and radio network infrastructure as efficiently as possible. RRM algorithms at the radio interface such as power control, interference management, admission control, resource reservation for mobility management, load control, channel allocation..., determine how the available radio resources of the system must be used and shared among the different users in an efficient way. In all the cases, the objective is to maximize the system spectral efficiency, while quality of service and grade of service requirements should be above a certain level.

The availability of positioning information in user stations can be exploited to design more advanced implementations of these Radio Resource Management strategies, thus increasing the efficiency of the cellular access networks (UMTS, IEEE 802.16...) and mobile ad-hoc networks (MANETs). In order to design even more efficient algorithms, location information can be combined with information of the environment topology (e.g. road network for tracking vehicles, presence of buildings or obstacles, etc.) and with statistic information (e.g. probability of different paths).

The increasing popularity of GPS (Global Positioning System) and the E-911 ruling issued by Federal Communications Commission (FCC), requiring the accurate localization of mobile callers requesting emergency services via 911 by the operators of mobile communication networks, motivated the integration of localization systems within mobile cellular networks. This encouraged both the research and development of location systems based on the information already available on the cellular networks (based on received power or time of arrival estimations between the mobile terminals and the base stations) and the research on the possible use of the location information on Radio Resource Management. Some proposals can be found in the literature since one decade, although research on the development of location-aware RRM algorithms for more efficient operation of wireless networks has gained an increasing interest with new and most sophisticated applications. Some examples of RRM procedures that are suitable to be enhanced are:

- Handover management and admission control: In general, the decision to perform a handover is made on the basis of received signal strength or link quality information. The use of positioning information allows a more accurate selection of the crossover point (avoiding the

ping-pong effect and reducing the dropping probability) and a better selection of the destination base station (reducing the number of handovers needed), resulting in an increase of the throughput and a reduction of the signalling load.

- **Resource reservation for mobility management:** Provision of QoS in the connection level focuses on developing strategies to minimize the forced termination of handoff calls and the risk of unnecessary block of new calls. In general, adaptive reserve of resources for handoff connections, based on the estimated position, movement and the desired QoS for each class of traffic associated to mobiles stations are desirable. Reservation of resources and mobile's call arrival prediction are closely related. The knowledge of the position and trajectory of a mobile allows an earlier detection of the need of the handover and therefore the reservation of resources in advance, thus reducing the handover dropping probability.
- **Load control and balance:** Knowledge of the position and trajectory of a mobile can be used to predict both the arrival of calls in handover and the amount of time that a call is going to stay in the cell (dwell time). Furthermore, in case of congestion of one of the cells, knowledge of the position and trajectory of each mobile would be helpful in order to decide which mobiles are more likely to be reallocated and to which cells should be allocated, thus balancing traffic load among the neighbour cells.
- **Resources allocation and interference management:** Location-awareness can be used to design enhanced channel allocation protocols in TDMA, FDMA and CDMA systems, reducing the co-channel inference and increasing the bandwidth efficiency. For example, taking advance of fractional frequency reuse schemes, a set of channels can be reserved to be exclusively used by cell-border users, which are more likely to suffer degradation due to interference. On the cell-border channels a reuse factor higher than 1 (e.g. of 3) is applied, while the rest of the channels can be used with a reuse factor of 1 by all the cell-centre users, as they are not so sensitive to interference.

The new concepts and algorithms for radio resources management with location awareness in wireless/cellular networks is specifically studied within Task 4.5. In D4.5.1 [22] the possible applications of location awareness in cellular and wireless networks are analyzed, and in D4.5.2 [23] specific algorithms and strategies are proposed that take advance of location-awareness.

2.3 Policy-Dependent distance distribution in linear multi-hop ad hoc networks

It has been shown that hopping policy in terms of closest, furthest and random hop strategy has a strong impact of the performance of wireless ad hoc networks regarding for instance capacity. In [24] the authors obtain better transmission capacity results when using closest neighbor strategy than choosing furthest hop policy. However, in [25] the costs and efficacy of relay selection was analyzed with the outcome that furthest neighbor relay selection is less sensitive to the number of contending nodes compared to hopping to the closest neighbor. This indicates that the relay selection overhead can be reduced by applying furthest neighbor selection. Random hopping strategies are considered in flooding and localization applications where the positions of sensor nodes are unknown. In [26] the authors introduce an efficient localization algorithm for multi-hop ad hoc networks allowing accurate self-localization where packets are forwarded to random nodes which act as relay nodes. The examples show that the choice of the hopping policy is a matter of the considered application.

What is generally true is that the number of hops has an impact on the time required for packets to reach a certain destination, while the hop length strongly impacts on the reliability of the communication. Hence, in order to quantify costs, delay and accuracy in multi-hop wireless ad hoc networks a detailed study of policy-dependent distance distribution is required leading to a challenging task. As the random deployment of nodes in ad hoc networks yields random inter-sensor distances and correlation in the random distances on a hop-by-hop basis the relation between hop distance and Euclidian distance cannot be obtained by using simple geometric calculations leading to a required statistical study. Furthermore, especially for planar networks the additional problem arises that hops not always occur on a straight line from source to destination leading to intractable expressions due to the swing problem.

In [27] the authors derive distance distributions for linear networks based on gaussian approximation being inaccurate for few hops. Whereas, the authors of [28] present a recursive expression for the distance distribution in planar networks which is not tractable for many hops.

In this work we obtain simple and clear expressions for the distance distribution in linear ad hoc networks and derive closed-form formulae for the expected number of hops by considering asymptotic lower bounds to eliminate correlations. Later, the results can be used for two dimensional networks to map the linear results and eliminate the swing problem. Using the derived distributions lower bounds on the expected number of hops required to reach a given Euclidean distance under each hopping policy are obtained in simple closed-forms. The expressions are found to be tight compared to experimental results obtained by simulations. The results indicate that the number of hops linearly depends on the distance with slope determined by the policy. The evaluation of the probability distribution of N given an Euclidean distance D implies that for a sufficient large distance our proposed method of using the average number of hops delivers accurate results compared to simulations.

In 2.3.1 we introduce the system model and its general parameters and derive the single-hop and multi-hop pdf for each routing policy. In 2.3.2 we derive analytically the expected progress per hop and obtain simple closed-form expression for the average number of hops. We use these results and show how to obtain simply the probability distribution $P(N|D)$ of the number of hops N given a certain distance D to the destination in 2.3.3. In 2.3.4 we verify our analytical results by simulations.

2.3.1 Single and multi-hop distances

We consider a linear multi-hop wireless sensor network with a source node, a destination node and N relay nodes. Let x_i with $i = 0 \dots N$ denote the location of the nodes where $x_0 = 0$ is the source's location and $x_N = D$ the destination's location, respectively. In the following, we assume $\{x_i\}_{i=0}^N$ to be independently and uniformly distributed random variables on $(0, D)$. Given a fixed transmission range R equal for all nodes, node $i-1$ and i are connected if their distance is equal to $r_i = |x_i - x_{i-1}| \leq R$.

Due to the independent and uniform deployment of the nodes, the occurrence probability of a node can be modeled as a one dimensional PPP. For our considerations we assume the product of the node density and radio range λR to be sufficient large such that there exists a path from source to destination. This assumption is feasible, since our goal is to use the pdf results of linear networks for dense planar networks where the probability that there exists a path from source to destination is sufficiently high.

We further assume that the next hop always occurs into the direction of the destination node. The source node triggers the transmission by sending the packet to a relay node being in range. In the following analytical considerations we distinguish between three different routing strategies in terms of random, closest and furthest hop as the choice of a certain hop policy affects the statistics of the distance distribution. The last hop from x_{N-1} to x_N is not affected by the routing strategy. Once a node in range of the destination receives the packet the next hop will certainly reach the destination.

First, we calculate the pdf by deriving the cdf of the single-hop distance. Hence, we are able to calculate the expected progress per hop and the expected number of hops given the Euclidian distance D .

2.3.1.1 Single-hop statistics

- **Random hop:** Figure 44 (a) depicts the random hop strategy where each transmitting node chooses randomly a relay node in range. As the nodes are distributed uniformly the cdf $F^r(r_i)$ and pdf $f^r(r_i)$ of the random hop strategy can be expressed by:

$$\begin{aligned} F^r(r_i) &= \frac{r_i}{R}, \\ f^r(r_i) &= \frac{1}{R}, \quad 0 \leq r_i \leq R. \end{aligned} \tag{17}$$

Hence, in case of random hops we obtain uniform and independent distributions. Note, that in case of random hops the node density λ does not affect the statistics as we assume that there is always a relay node in range. Thus, the transmitting node picks one of the nodes in range as relay leading to a process which is independent of λ .

- **Closest hop:** Figure 44 (b) shows the single-hop distance in the case where routing is performed to the closest relay indicating that all nodes have to be considered to reach the destination. In order to calculate the statistics we use the characteristics of the PPP as it describes the probability of the occurrence of k nodes with density λ within a certain range r by [30]:

$$P(N = k) = \frac{e^{-\lambda r} (\lambda r)^k}{k!} \tag{18}$$

Hence, the probability of having at least one node in r_i is given by $1 - e^{-\lambda R}$ yielding the cdf and its pdf $f^c(r_i)$ expressed by:

$$F^c(r_i) = \frac{1 - e^{-\lambda R}}{1 - e^{-\lambda r_i}},$$

$$f^c(r_i) = \frac{\lambda e^{-\lambda r_i}}{1 - e^{-\lambda R}}, \quad 0 \leq r_i \leq R,$$

(19)

where the denominator $\int_0^R f^c(r_i) dr_i = 1 - e^{-\lambda R}$ denotes the restriction to R . Due to the fact that every node has to be considered as a relay in the closest hop policy the outcome in terms of the cdf and pdf respectively is independently distributed.

- **Furthest hop:** The minimum path of a source destination pair relies on the furthest hop strategy as the most distant node acts always as relay node. It is the most investigated case in literature and its single-hop statistic is described in [29]. Figure 44 (c) indicates that the hop to the furthest node yields a vacant segment r_i^e being empty which has to be considered in terms of a condition. Hence, the cdf can be calculated like in the case of closest hop times the probability of having no nodes in r_i^e . Its cdf and pdf are expressed by:

$$F^f(r_i) = \frac{e^{-\lambda R} (e^{\lambda r_i} - e^{\lambda r_{i-1}^e})}{1 - e^{-\lambda(R-r_{i-1}^e)}},$$

$$f^f(r_i) = \frac{\lambda e^{-\lambda(R-r_i)}}{1 - e^{-\lambda(R-r_{i-1}^e)}}, \quad r_{i-1}^e \leq r_i \leq R.$$

(20)

Obviously, we obtain a recursive expression where the next hop distance is a function of the previous empty segment r_{i-1}^e .

For sufficient large λR it follows that $r_{i-1}^e \ll R$ and allows us to neglect r_{i-1}^e . In the following we will consider $r_{i-1}^e = 0$ and $r_{i-1}^e = E[r_i^e]$. The latter case relies on the idea that the empty gap can be approximated by its mean value to avoid correlations.

2.3.1.2 Multi-hop statistics

The multihop distance is defined by the sum of the single-hop distances r_i and is given by

$d_N = \sum_{i=1}^N r_i$. In order to obtain the statistics of the multi-hop distance we focus on the pdf of the sum of independent random variables which can be calculated by the convolution of the single-hop pdf

$$\int_0^{d_N} f(r) f(d_N - r) dr \quad [30].$$

In the following we will introduce the pdf of the multi-hop distance for the different routing strategies.

- **Random hop:** Since we deal with uniformly and independently distributed random variables the sum of them leads to the so-called Irwin-Hall distribution given by:

$$f^r(d_N) = \frac{\sum_{k=0}^N (-1)^k \binom{N}{k} (d_N - kR)^{N-1} \text{sgn}(d_N - kR)}{2R^N \Gamma(N)}, \quad 0 \leq d_N \leq NR. \quad (21)$$

where $\Gamma(N) = (N-1)!$ denotes the gamma function. The special case for $N = 2$ leads to the triangular distribution as we convolve two uniformly distributed random variables. Due to the Central Limit theorem the distribution converges to the Normal distribution for increasing N .

- **Closest hop:** In the closest hop case the single-hop distribution relies on the PPP which has an exponential distribution. Hence, the pdf of the sum yields an Erlang distribution expressed by:

$$f^c(d_N) = \frac{\lambda^N d_N^{N-1} e^{-\lambda d_N}}{\Gamma(N)(1 - e^{-\lambda R})^N}, \quad 0 \leq d_N \leq NR. \quad (22)$$

Like the random hop strategy the distribution converges to the Normal distribution as we deal with iid. random variables r_i .

- **Furthest hop:** In order to determine the multi-hop statistics we focus on the distribution of the vacant segment r_i^e . Due to the fact that $d_N = NR - d_N^e$, $f^f(d_N)$ can be expressed by $f^f(d_N) = f_{d_N^e}^f(NR - d_N)$.

In case of $r_{i-1}^e = 0$ the vacant segment distribution corresponds to the closest hop distribution.

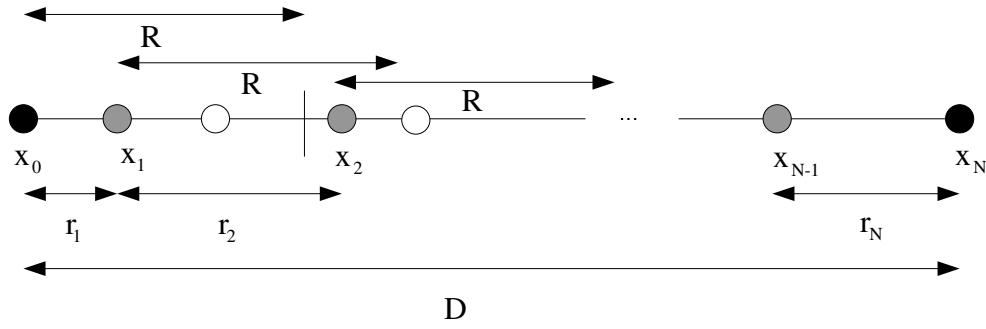
Hence, $f^f(d_N) = f_{d_N^e}^f(NR - d_N)$:

$$f^f(d_N) = \frac{\lambda^N (NR - d_N)^{N-1} e^{-\lambda(NR - d_N)}}{\Gamma(N)(1 - e^{-\lambda R})^N}, \quad 0 \leq d_N \leq NR. \quad (23)$$

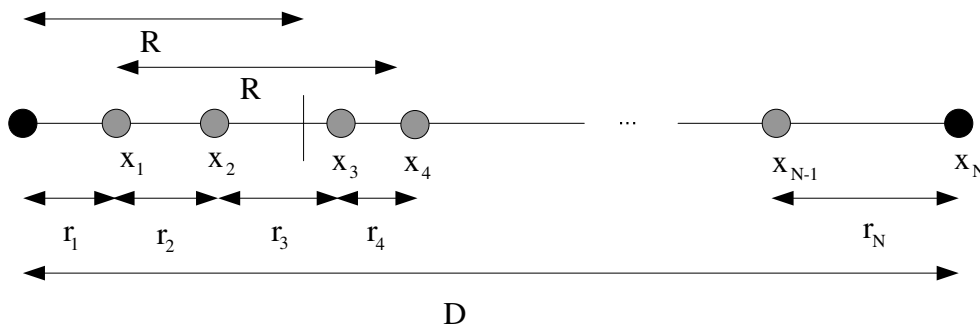
For the case where we assume $r_{i-1}^e = E[r_i^e]$ the distribution is similar. However, due to the definition range of r_i with $R - r_{i-1}^e \leq r_i \leq R$ where $r_0^e = 0$ we can express the multi-hop pdf by:

$$f^f(d_N) = \frac{\lambda^N (NR - d_N)^{N-1} e^{-\lambda(NR - d_N)}}{\Gamma(N)(1 - e^{-\lambda R})(1 - e^{-\lambda(R - E[r_i^e])})^{N-1}}, \quad NE[r_i^e] \leq d_N \leq NR. \quad (24)$$

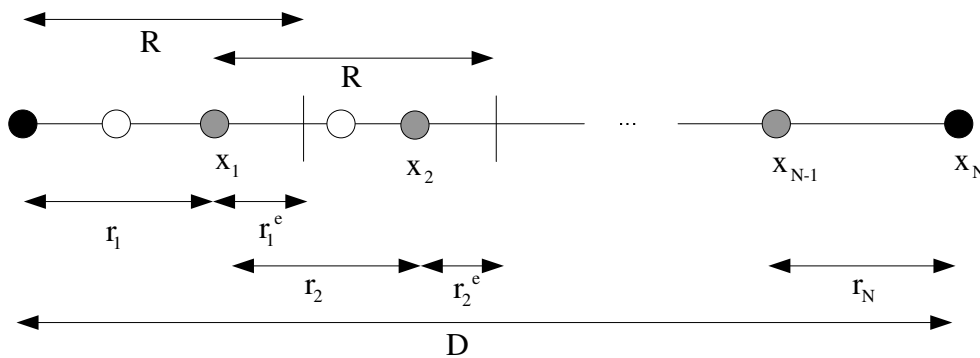
The denominator of the pdf consist of $(1 - e^{-\lambda R})(1 - e^{-\lambda(R - E[r_i^e])})^{N-1}$ implying that for $i = 1$ the range of r_1 is in range of $0 \leq r_1 \leq R$ and the range for $i > 1$ corresponds to $r_{i-1}^e \leq r_i \leq R$. Assuming $r_{i-1}^e = E[r_i^e] = 0$ equation (24) results in equation (23) again.



(a) Random hop



(b) Closest hop



(c) Furthest hop

Figure 44: Illustration of different routing strategies: (a) random, (b) closest and (c) furthest

2.3.2 Average number of hops

The expected number of hops can be calculated by the assumption that every single-hop distance r_i is identically distributed with a certain mean $E[r_i] = E[r]$ which we derive in the following for different hopping strategies. Hence, we determine the mean number of hops given an Euclidian distance generally by $E[N] = \frac{D}{E[r]}$.

- **Random hop:** The expected progress per hop for random policy is given by:

$$E^r[r] = \int_0^R r f^r(r) dr = \frac{R}{2}. \quad (25)$$

- **Closest hop:** The expected progress per hop is calculated analogously as in the random case and given by:

$$E^c[r] = \int_0^R r f^c(r) dr = \frac{1 - e^{-\lambda R} (\lambda R - 1)}{\lambda (1 - e^{-\lambda R})}. \quad (26)$$

The characteristic of $E^c[r]$ is depicted in Figure 45 (a) and indicates the asymptotic behavior. By increasing λ the mean hop distance is decreased as the number of nodes increases and with this automatically their distances.

Note, that for the closest hopping policy the simple consideration that every node in the network serves as a relay node leads to the fact, that the number of hops is always equal to the number of nodes in the network. Hence, by calculating the total number of nodes in the network given by the PPP we obtain automatically the number of hops.

- **Furthest hop:** We obtain for $E^f[r]$ when neglecting r_{i-1}^e :

$$E^f[r] = R - \frac{1 - e^{-\lambda R} (\lambda R - 1)}{\lambda (1 - e^{-\lambda R})}. \quad (27)$$

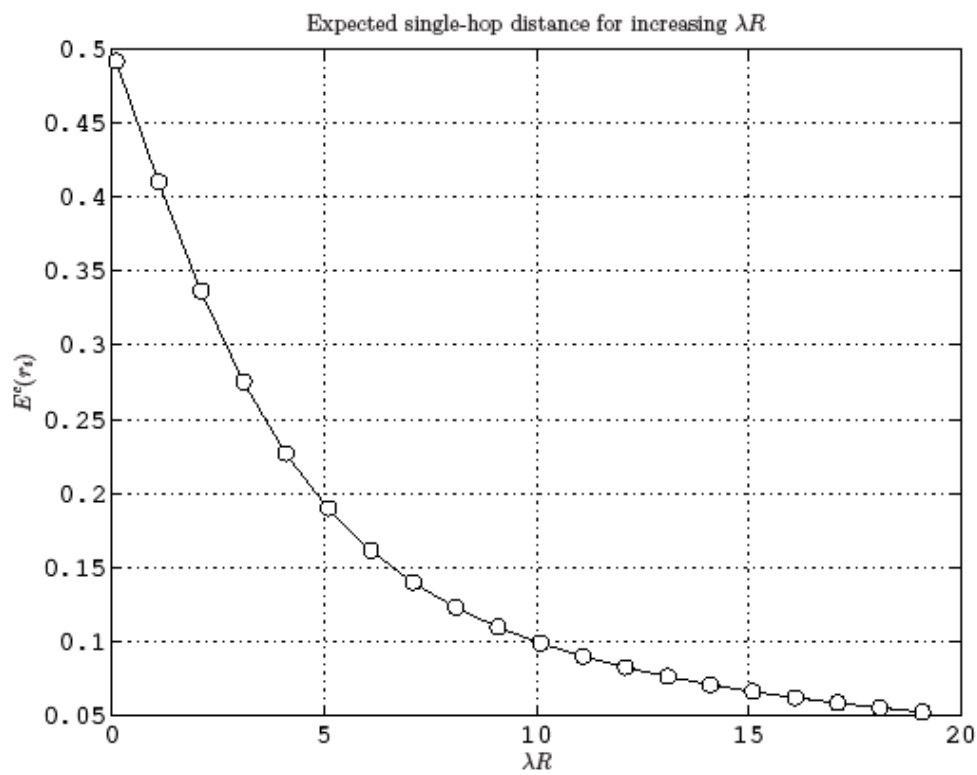
Since $r_i = R - r_{i-1}^e$ and the distribution of the vacant segment becomes equal to the closest hop case and we obtain the mean value by subtracting R from the expected value of the closest hop case.

The expected value $E^f[r]$ when approximating r_{i-1}^e by its mean leads to a numerically solvable expression given by:

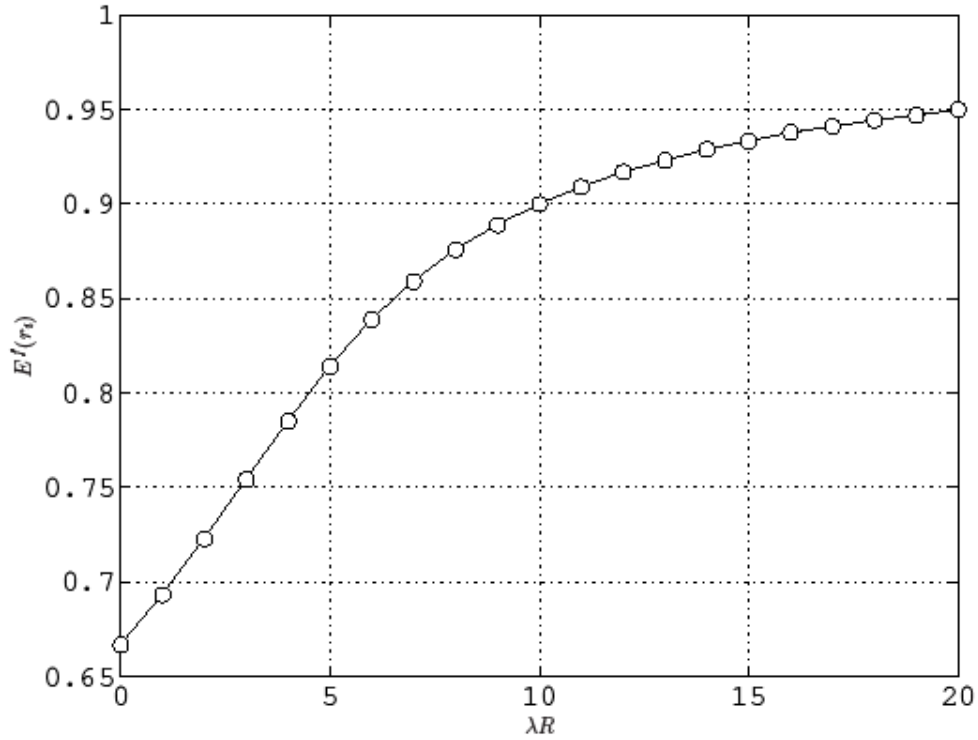
$$\ln\left(1 - \frac{\lambda E^f[r]}{\lambda R - \lambda E^f[r] - 1}\right) - \lambda E^f[r] = 0$$

(28)

Hence, for certain λR we can calculate $E^f[r]$ numerically. Figure 45 (b) shows the characteristics of the expected value and implies the asymptotic behavior. By increasing λR the mean hop progress converges to the maximum transmission range. It must have the opposite characteristic compared to the closest hop case.



(a) Closest hop strategy



(a) Furthest hop strategy

Figure 45: Characteristic of the expected single-hop distance for (a) closest and (b) furthest hop strategy

2.3.3 Probability distribution of the number of hops

There exists some work in the literature investigating how to obtain the probability distribution of the number of hops. One method for instance shown in [27] makes use of the multi-hop probability density function which is assumed to be gaussian. They derived the expression of $P(N|D)$ by using Baye's Rule. Their analytical expression is given by:

$$P(N|D) = \frac{\int_{D-R}^D f_{d_{N-1}}(x) dx \prod_{j=1}^{N-2} \int_0^{D-R} f_{d_j}(x) dx}{\sum_{i=N_{\min}}^{N_{\max}} \int_{D-R}^D f_{d_{i-1}}(x) dx \prod_{j=1}^{i-2} \int_0^{D-R} f_{d_j}(x) dx}, \quad (29)$$

where $f_{d_{N-1}}(x)$ denotes the multi-hop pdf of the N th-1 hop. The expression indicates that $P(N|D)$ consists of two parts. First the probability that the N th-1 hop falls into the range of the destination and the probability that all N th-2 hops do not normalized by the sum of all. Hence, the product of the integral over $f_{d_j}(x)$ for all N th-2 hop must be computed leading to a complex calculation. Thus, in the following we will present a simple method to obtain $P(N|D)$ for each

hopping strategy by making use of the knowledge that the distribution of the total number of nodes in the whole network is given by the Poisson process.

In order to determine the probability distribution of the number of hops N given a distance D we first refer to the closest hop policy where we know that the number of hops is supposed to be equal to the number of nodes in the network as we have to consider each single node when hopping to the destination. Thus, this leads to a trivial solution as the number of nodes in the network rely on the Poisson process which gives us the probability of having k nodes within a certain range D given a density λ . Hence, the number of nodes in our network follows this distribution and can be expressed by $P(N = k) = \frac{e^{-\lambda r} (\lambda r)^k}{k!}$. As we assumed the network to be fully connected by we can expect the

probability distribution of the number of hops for the closest hop strategy $P^c(N | D)$ to be equal to the Poisson process. However, note that the Poisson process delivers non-zero values for all k . In order to be able to use the Poisson process to determine $P^c(N | D)$ the minimum number of hops given by $N_{\min} = \frac{D}{R}$ has to be considered. For $N < N_{\min}$, $P^c(N | D)$ is supposed to be zero and a normalization is required. Finally, the probability distribution $P^c(N | D)$ can be given by:

$$P^c(N | D) = \frac{e^{-\lambda D} (\lambda D)^N}{N! \sum_{i=N_{\min}}^{N_{\max}} P(i | D)}, \quad N \geq N_{\min}. \quad (30)$$

For the random and furthest case the same distribution must hold though not all nodes act as relays. However, in order to determine $P(N | D)$ we consider the number of nodes bypassed at each hop which is actually a random variable but can be described by its average \bar{N}_B when assuming large number of hops. Hence, the total number of nodes in the network which is also a random variable and given by the Poisson process can be expressed by $N_N = N + \bar{N}_B$. This indicates that the number of hops is given by the total number of nodes with the known distribution scaled by a constant. Hence, we can obtain the probability distribution for the random and furthest policy by using the distribution of the closest hop policy and the scaling factor:

$$P^{r,f}(N | D) = \frac{1}{a} P^c\left(\frac{N}{a} | D\right), \quad N \geq N_{\min}, \quad (31)$$

where $a = \frac{1}{1 + \bar{N}_B}$. Note, that the mean number of bypassed nodes is different for each policy and can

be determine by calculating the mean of the Poisson process for the expected progress per hop given
in

the previous section according to each strategy. Thus, the mean number of bypassed nodes can be given by:

$$\overline{N}_B = E\left[\frac{e^{-\lambda E[r]} (\lambda E[r])^{N_B}}{N_B!}\right]$$

(32)

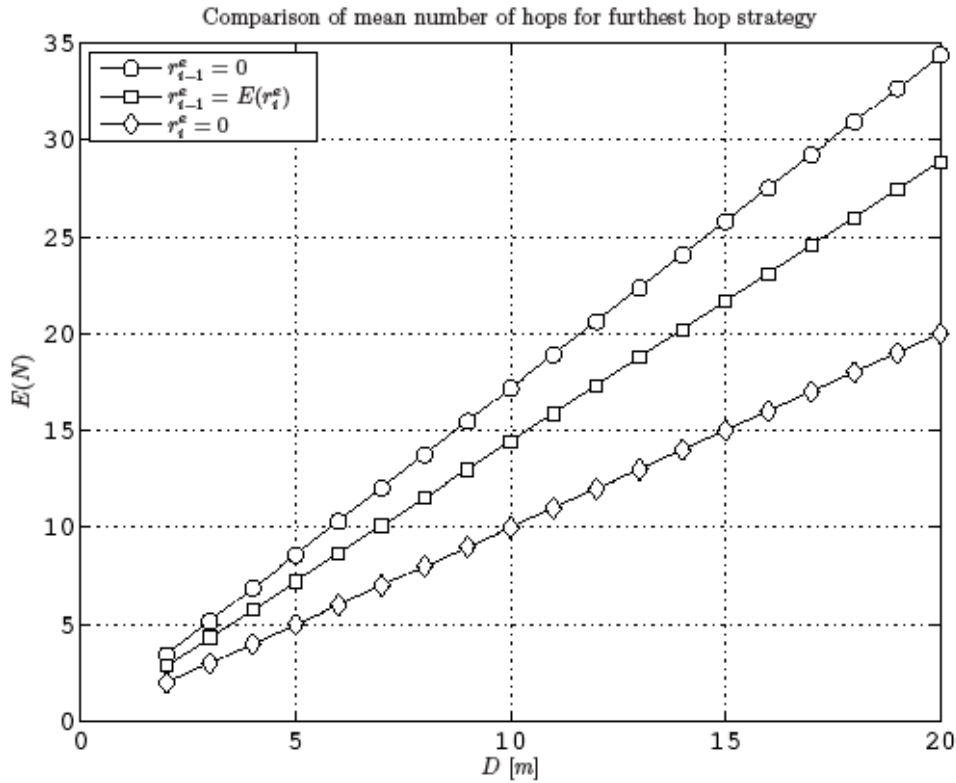
2.3.4 Evaluation and simulation results

In Figure 46 (a) the mean number of hops versus the Euclidean distance is evaluated for the independence assumption $r_{i-1}^e = 0$, for the case where $r_{i-1}^e = E[r^e]$ and the trivial case where we assume that hops always occur to the maximum range $r_i^e = 0$. Note, that for the trivial case where $r_i^e = 0$ the mean number of hops corresponds to $N_{\min} = \frac{D}{R}$ which stands for the lowest bound. The upper bound is given by the assumption that $r_{i-1}^e = 0$ as we reach the smallest progress per hop for this case. Finally, the case where $r_{i-1}^e = E[r^e]$ leads to a mean number of hops in between the upper and lower bound.

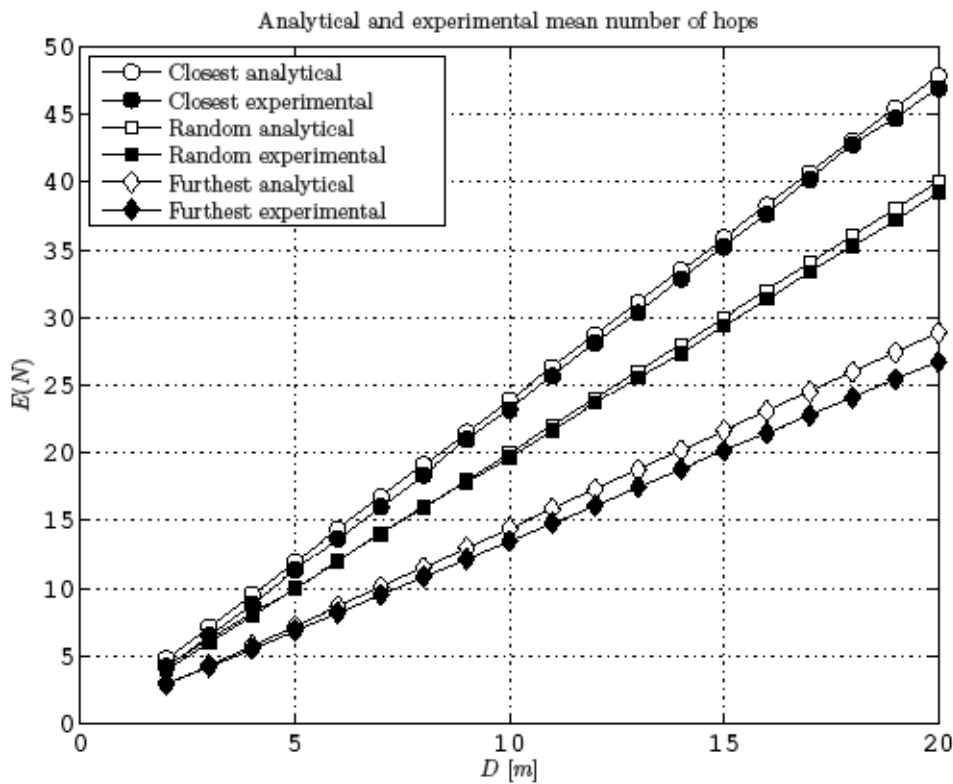
Figure 46 (b) depicts the analytical evaluation of the mean number of hops for the different routing strategies compared to experimental results obtained by simulations. The experimental results are obtained by performing $K=10000$ simulation runs per point.

In general, the analytical results are very similar to the experimental results.

For the evaluation results of $P(N | D)$ we refer to Figure 47 where the experimental and the analytical results for each hopping strategy are depicted for a Euclidean distance of $D = 10$ m. The diamond markers are the probability of N for the analytical case mapped onto the experimental results depicted as boxes with a mean value and the variance of the simulation. The results indicate that for a sufficiently large node density and distance the proposed method yield accurate results compared to results obtained by simulations even for the furthest and random case where we consider the number of bypassed nodes by its average value. Hence, we showed a very easy and low complex way to calculate the probability distribution $P(N | D)$ accurately.

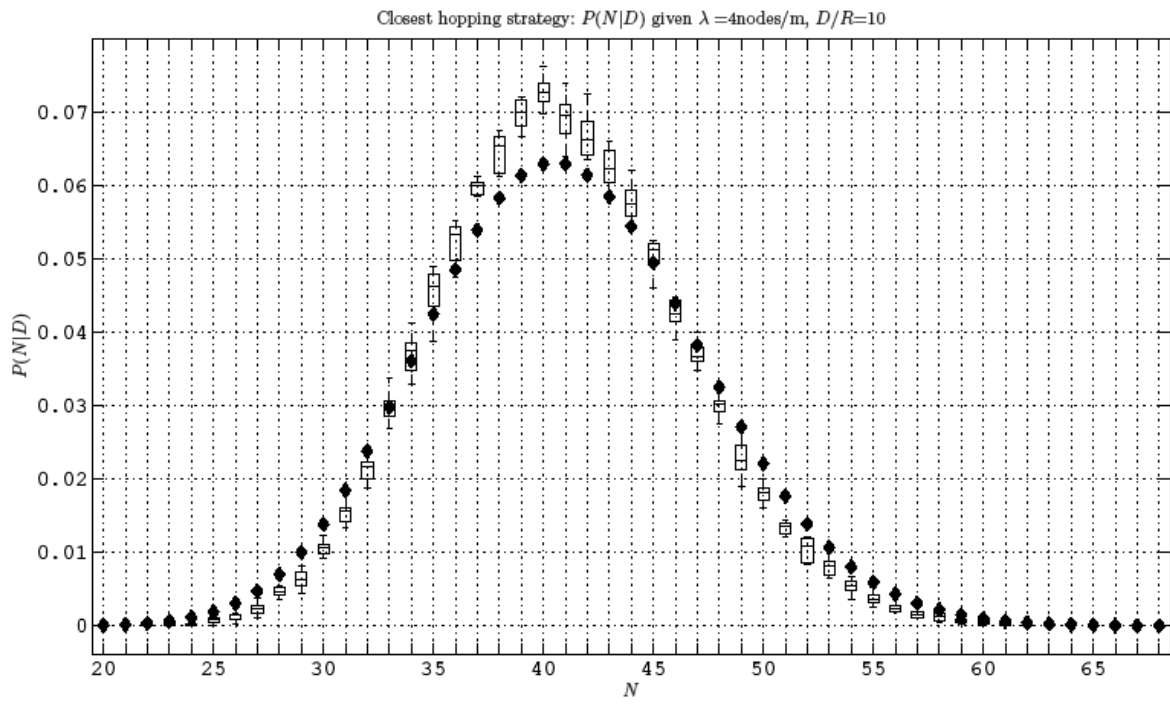


(a) Mean number of hops for different assumption of vacant segment

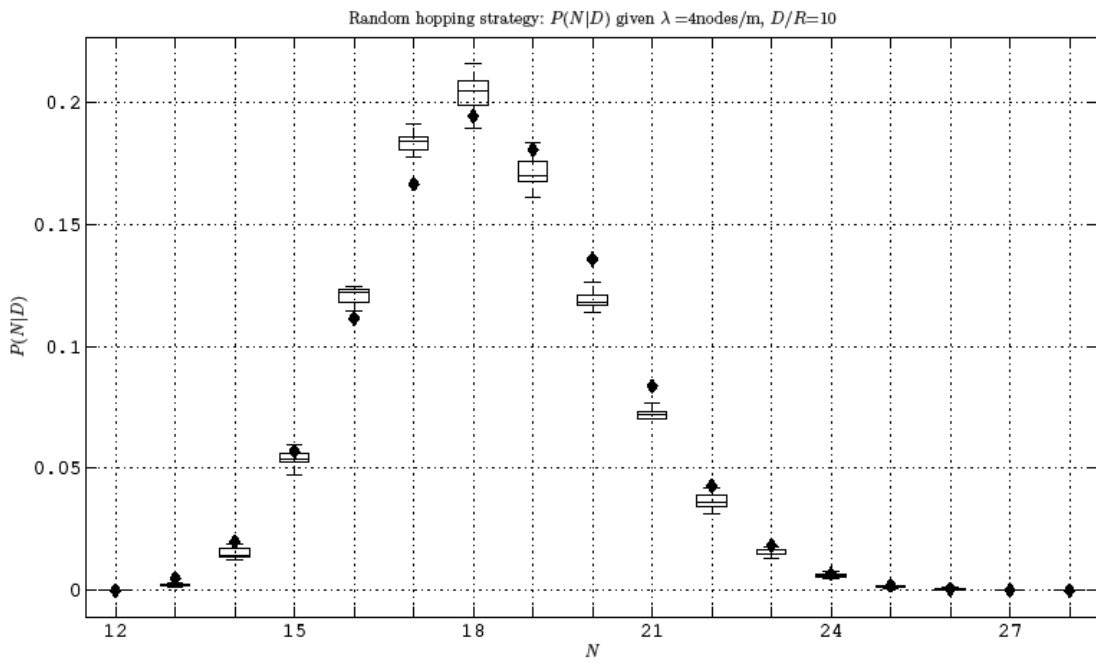


(a) Comparison of mean number of hops analytical vs. experimental for different strategies

Figure 46: Evaluation of the mean number of hops (a) different assumptions for furthest hop policy and (b) comparison analytical vs. experimental for all strategies



(a) Closest hop strategy



(b) Random hop strategy

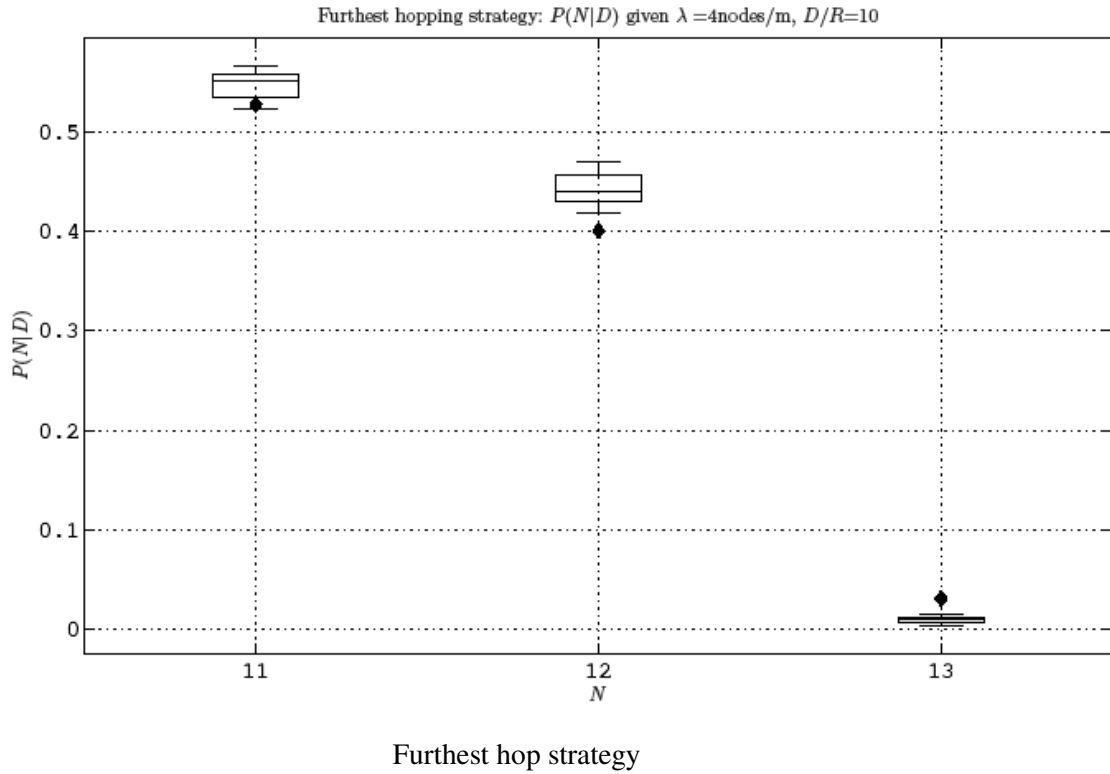


Figure 47: Evaluation of the probability distribution of the number of hops given a fixed distance for all hopping policy

2.3.5 Conclusion

Finally we presented closed-form expressions for the single-hop statistics of the distance distribution in linear wireless sensor networks for different routing policies in terms of the pdf and expected values for the progress per hop and number of hops respectively. Furthermore, we exploit the single-hop information to obtain the pdf for multi-hop distance distribution by applying convolution. We verify our analytical results by simulations and show that the mean number of hops obtained by our analytics is highly consistent with the experimental results. Furthermore, we tested our proposed method to calculate the probability distribution of the number of hops given a Euclidean distance and showed that it fits quite good to the experimental results when assuming a large distance where the number of hops are sufficient large. This can be explained by the choice of the number of bypassed nodes which is actually a random variable but was replaced by its average value.

Using the results for one dimensional networks and map them to two dimensional ones is our immediate next step. The obtained results can further be used to quantify e.g. the communication costs of multi-hop self-localization algorithms and better evaluate the total cost of relay selection. The information can also be exploit to enhance the work done in [24] by analyzing the aggregate information efficiency taking into account the number of hops.

References

- [1] URL of EUWB consortium: <http://www.euwb.eu>
- [2] P. Krishnamurthy, H. Karimi, "Telegeoinformatics for Efficient Resource Allocation and Protocol Development in Wireless Networks", IEEE Vehicular Technology Conference, Boston, MA, September 2000.
- [3] Bovelli, S., Leipold, F.: "Scenario description for public transport applications", EUWB Deliverable D8a.1
- [4] Bovelli, S., Leipold, F.: "Requirements for public transport applications", EUWB Deliverable D8a.2
- [5] Hasch, J.: "Scenario description for automotive environment applications", EUWB Deliverable D8b.1
- [6] Hasch, J.: "System parameters for automotive environment applications", EUWB Deliverable D8b.2
- [7] Van Daele, B., Hafezi, P.: "Scenario Descriptions for Localisation Application for Home Audio Systems", EUWB Deliverable D8c.6
- [8] Hafezi, P., Van Daele, B.: "System parameters and requirements for localization/synchronization for home audio applications", EUWB Deliverable D8c.7
- [9] "Enhanced dissemination methods and evaluation" D4.2.2 final version, September 2009, EUWB (IST FP7-215669), public deliverable.
- [10] IEEE 802.15.4 standard, "Part 15.4: Wireless Medium Access Control (MAC) and Physical Layer (PHY) Specifications for Low-Rate Wireless Personal Area Networks (LR-WPANs)"
- [11] "LDR-LT platform requirements, feasibility analysis and specification" D7.1.1a final version, September 2008, EUWB (IST FP7-215669), public deliverable.
- [12] D. Macagnano, G. Destino, F. Esposito, and G. T. F. de Abreu, "MAC Performances for Localization and Tracking in Wireless Sensor Networks", In Proc. WPNC'07, Hannover.
- [13] "Enhanced LT system- PHY, MAC and Network layers (final)" D3a-2.3 final version, June 2008, PULSERS Phase II (IST FP6-027142), public deliverable.
- [14] B. Denis and N. Daniele, "NLOS Ranging Error Mitigation in a Distributed Positioning Algorithm for Indoor UWB Ad Hoc Networks", in Proc. IEEE IWWAN'04., pp. 356-360 Oulu, May-June 2004
- [15] B. Denis, J.B. Pierrot and C. Abou-Rjeily, "Joint Distributed Time Synchronization and Positioning in UWB Ad Hoc Networks Using TOA", IEEE Trans. on MTT, Special Issue on Ultra Wideband, Vol. 54, Is. 4, Part 2, pp. 1896-1911, April 2006.
- [16] F. Daum, "Nonlinear filters: beyond the Kalman filter", IEEE Aerospace and Electronic Systems Mag., vol. 20, no. 8, pp. 57-69, Aug. 2005.
- [17] KFilter library project website: <http://kalman.sourceforge.net/>
- [18] D. Macagnano and G. T. F. de Abreu, "Tracking Multiple Targets with Multidimensional Scaling," in Wireless Personal Multimedia Communications, Sep. 2006
- [19] "Implementation of the enhanced LT engine with mobility management (LDR and HDR)" D4.3.2a final version, September 2009, EUWB (IST FP7-215669), public deliverable.
- [20] F. Gustafsson, F. Gunnarsson, N. Bergman, U. Forssell, J. Jansson, R. Karlsson, and P.-J. Nordlund, "Particle filters for positioning, navigation and tracking", IEEE Transactions on Signal Processing, Feb 2002.
- [21] A. M. Johansen. SMCTC: Sequential Monte Carlo in C++. Journal of Statistical Software, 30(6):1-41, April 2009.

- [22] “Analysis of location awareness in wireless/cellular networks” D4.5.1 final version, June 2009, EUWB (IST FP7-215669), public deliverable.
- [23] “Algorithms and strategies for communication systems with location awareness (initial)” D4.5.2a final version, March 2010, EUWB (IST FP7-215669), public deliverable.
- [24] P. Nardelli, G. Abreu, “On hopping strategies for autonomous multi-hop wireless networks, IEEE Global Telecommunications Conference (GLOBECOM), 2009.
- [25] C. Lima, G. Abreu, “Analysis of contention-based relay selection mechanism in autonomous multi-hop networks”, ITW 2009, Volos, Greece.
- [26] S. Severi, G. Abreu, G. Destino, D. Dardari, “Efficient and accurate localization in multihop networks”, Asilomar Conference on Signals, Systems and Computers, 2009.
- [27] S. Vural and E. Ekici, “Probability distribution of multi-hop-distance in one-dimensional sensor networks”, The International Journal of Computer and Telecommunications Networking, Volume 51 , Issue 13, September 2007.
- [28] X. Ta, G. Mao and B.D.O. Anderson, "On the probability of k-hop connection in wireless sensor networks", IEEE Communication Letters, Vol. 11, No. 9, September, pp. 662-664, 2007.
- [29] Y. C. Cheng and T. G. Robertazzi, “Critical Connectivity Phenomena in Multihop Radio Models”, Communications, IEEE Transactions on, Volume 37, Issue 7, Jul 1989, p.:770 - 777.
- [30] S. Ross, “A First Course in Probability”, Prentice-Hall, 2005.

Acknowledgement

The EUWB consortium would like to acknowledge the support of the European Commission partly funding the EUWB project under Grant Agreement FP7-ICT-215669, [1].